

DEVELOPMENT OF FRAGILITY CURVES OF MULTI-STORY BUILDINGS WITH SOLID AND PERFORATED SHEAR WALL

A DISSERTATION

SUBMITTED IN PARTIAL FULFILLMENT OF THE REQUIREMENTS

FOR THE AWARD OF THE DEGREE

OF

MASTER OF TECHNOLOGY
IN
STRUCTURAL ENGINEERING

Submitted by

SUDHIR KUMAR BAGHEL

2K21/STE/21

Under the supervision of

Mr. G.P. AWADHIYA

(Associate Professor)



**DEPARTMENT OF CIVIL ENGINEERING
DELHI TECHNOLOGICAL UNIVERSITY**

(Formerly Delhi College of Engineering)

Bawana Road, Delhi-110042

MAY, 2023

M. Tech. Structural Engineering

Sudhir Kumar Baghel

2023

DELHI TECHNOLOGICAL UNIVERSITY
(Formerly Delhi College of Engineering)
Bawana Road, Delhi- 110042

CANDIDATE'S DECLARATION

I, **Sudhir Kumar Baghel**, 2K21/STE/21 student of MTech Structural Engineering, hereby declare that the Project Dissertation titled “**Development of Fragility Curves of Multi-Story Buildings with Solid and Perforated Shear Wall**”, which is submitted by me to the Department of Civil Engineering, Delhi Technological University, Delhi in partial fulfillment of the requirement for the award of the degree of Master of Technology, in original and not copied for any source without proper citation. This work has not previously formed the basis for the award of any Degree, Diploma Associateship, Fellowship, or other similar title or similar recognition.



Place: Delhi
Date:

SUDHIR KUMAR BAGHEL

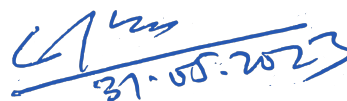
DEPARTMENT OF CIVIL ENGINEERING
DELHI TECHNOLOGICAL UNIVERSITY
(Formerly Delhi College of Engineering)
Bawana Road, Delhi-110042

CERTIFICATE

I hereby certify that the Project Dissertation titled “**Development of Fragility Curves of Multi-Story Buildings with Solid and Perforated Shear Wall**”, which is submitted by Sudhir Kumar Baghel, 2K21/STE/21, Department of Civil Engineering, Delhi Technological University, Delhi in partial fulfilment of the requirement for the award of degree the of Master of Technology, is a record of the project work carried out by the student under my supervision. To the best of my knowledge, this work has not been submitted in part or full for any degree or diploma to this university or elsewhere.

Place: Delhi

Date:



Mr. G.P. AWADHIYA

SUPERVISOR

Associate professor

Department of Civil Engineering

Delhi Technological University

Bawana road, Delhi - 110042

ACKNOWLEDGEMENT

I am overwhelmed in all humbleness and gratefulness to acknowledge my depth to all those who have helped me to put these ideas, well above the level of simplicity and into something concrete. I would like to express my special thanks of gratitude to my project supervisor Sh. G.P. Awadhiya who gave me the opportunity to do this wonderful project on the topic “Development of Fragility Curves of Multi-Story Buildings With Solid And Perforated Shear Wall”, which also helped me in doing a lot of research and learning the oddities. Any attempt at any level can't be satisfactorily completed without the support and guidance of the Faculties of Dept. of Civil Engineering, DTU, my parents, and friends.



SUDHIR KUMAR BAGHEL

ABSTRACT

This research study focuses on evaluating the seismic performance and vulnerability of different building models within a G+10-story reinforced concrete structure with complex geometry. The investigation specifically examines the effects of incorporating shear walls, including perforated shear walls, on the structural integrity and response under seismic loads. The objectives of the study include comparing the building models, analyzing top storey displacement and drift, assessing lateral displacement and drift reduction in both X and Y directions, and developing fragility curves for each model using pushover and time history methods.

The findings of the study reveal that the shear wall frame structure (Model B) exhibits significant improvements in reducing displacement and drift compared to the bare frame structure (Model A). The perforated shear wall frame structure (Model C) also demonstrates notable enhancements in seismic performance. While Model B generally outperforms Model C, Model C achieves reduced drift values at specific floor levels in the Y direction. The selection between Model B and Model C depends on project-specific requirements and design considerations.

The study underscores the effectiveness of shear wall frame structures in enhancing seismic performance and contributes to the advancement of resilient building designs in high seismic zones. The analysis highlights the superiority of Model B over Model A and Model C in reducing lateral displacement and drift. It also emphasizes the importance of

incorporating shear walls in frame structures and suggests that extending shear walls throughout the entire height of a building may not be necessary, leading to potential cost savings in construction.

The fragility curves developed for each model provide insights into their vulnerability and likelihood of damage or failure under different seismic events. The results show that Model A exhibits higher vulnerability compared to Model C, and Model C displays higher vulnerability compared to Model B, across various damage states specifically in slight, moderate, extensive, and collapse. Furthermore, Model A exhibits higher vulnerability compared to Model B, and Model B exhibits higher vulnerability compared to Model C, specifically in OP, IO, DC, LS, and CP damage states.

In conclusion, this research highlights the significance of shear wall frame structures in improving the seismic performance and fragility of buildings. The study's findings can inform decision-making processes in seismic design and contribute to the development of more resilient structures in earthquake-prone areas.

TABLE OF CONTENTS

CANDIDATE’S DECLARATION	i
CERTIFICATE	ii
ACKNOWLEDGEMENT	iii
ABSTRACT	iv
TABLE OF CONTENTS	vi
LIST OF FIGURES	viii
LIST OF TABLES	x
ABBREVIATIONS	xi
CHAPTER 1 INTRODUCTION	1
1.1 General	1
1.2 Seismic Fragility Curve	3
1.3 Pushover Analysis Method	4
1.4 Nonlinear time history analysis	5
1.5 Objectives of the Study	6
1.6 Organisation of the Thesis	7
CHAPTER 2 LITERATURE REVIEW	9
2.1 General	9
2.2 Literature Review	9
CHAPTER 3 METHODOLOGY	13
3.1 Problem Statement	13
3.2 Construction of pushover curves.	15
3.3 Development of fragility curves.	16
3.3.1 Development of fragility curves by pushover method.	16
3.3.2 Development of fragility curves by time history method.	17
CHAPTER 4 RESULTS AND DISCUSSIONS	19
4.1 Results	19
4.2 Discussions	26
4.3 Construction of Fragility Curves	29

CHAPTER 5 CONCLUSION	36
5.1 Conclusion	36
5.2 Scope of Future Work	38
APPENDICES	39
Appendix 1: Probability of exceedance calculation for pushover results.	41
Appendix 2: Pushover curve for different models.	41
Appendix 3: Probability of exceedance calculation for time history results.	43
REFERENCES	46

LIST OF FIGURES

Figure No.	Description	Page No.
1.1	Typical Fragility Curve.	3
3.1	Building plan (Source: Vaibhav Keshari [1])	13
3.2	Model A- Bare frame structure	14
3.3	Model B- Shear wall framed structure	14
3.4	Model C- Perforated shear wall frame structure	15
4.1	Lateral Displacement (mm) along X Direction for Push X case.	23
4.2	Lateral Displacement (mm) along Y Direction for Push X case.	24
4.3	Story Drifts along X Direction for Push X Results.	24
4.4	Story Drifts along Y Direction for Push X Results.	24
4.5	Lateral Displacement (mm) along X Direction for Push Y case.	25
4.6	Lateral Displacement (mm) along Y Direction for Push Y case.	25
4.7	Story Drifts along X Direction for Push Y Results.	25
4.8	Story Drifts along Y Direction for Push Y Results.	26
4.9	Base shear for different models.	26
4.10	Model A- Bare Frame.	30
4.11	Fragility curve for bare frame by pushover analysis.	30
4.12	Fragility curve for bare frame by time history method.	30
4.13	Model B- Shear wall structure.	31
4.14	Fragility curve for shear wall structure by pushover analysis.	31
4.15	Fragility Curve for shear wall structure by time history method.	31
4.16	Model B- Perforated Shear wall structure.	32
4.17	Fragility Curve for Perforated Shear wall by pushover analysis.	32
4.18	Fragility curve for perforated shear wall time history method.	32
4.19	Fragility Curve for Slight Damage for BF, SW and PSW.	33
4.2	Fragility Curve for Moderate Damage for BF, SW and PSW.	33

4.21	Fragility Curve for Extensive Damage for BF, SW and PSW.	33
4.22	Fragility Curve for Collapse Damage for BF, SW and PSW.	34
4.23	Fragility Curve of OP for BF, SW and PSW.	34
4.24	Fragility Curve of IO for BF, SW and PSW.	34
4.25	Fragility Curve of DC for BF, SW and PSW.	35
4.26	Fragility Curve of LS for BF, SW and PSW.	35
4.27	Fragility Curve of CP for BF, SW and PSW.	35
A.2.1	Pushover Curves for Bare Frame Structure in X and Y direction.	41
A.2.2	Pushover Curves for Shear wall Frame Structure in X and Y direction.	42
A.2.3	Pushover Curves for Perforated Shear wall Frame Structure in X and Y direction.	42

LIST OF TABLES

Table No.	Description	Page No.
3.1	Building Description	14
3.2	Load Description	14
3.3	HAZUS Damage state thresholds	17
3.4	Ssd and β Sds assumed as per HAZUS Manual.	17
4.1	Lateral Displacement (mm) along X Direction. (Push X Results)	19
4.2	Lateral Displacement (mm) along Y Direction. (Push X Results)	20
4.3	Story Drifts along X Direction. (Push X Results)	20
4.4	Story Drifts along Y Direction. (Push X Results)	21
4.5	Lateral Displacement (mm) along X Direction. (Push Y Results)	21
4.6	Lateral Displacement (mm) along Y Direction. (Push Y Results)	22
4.7	Story Drifts along X Direction. (Push Y Results)	22
4.8	Story Drifts along Y Direction. (Push Y Results)	23
A.1.1	Values for different parameters.	39
A.1.2	Probability of exceedance calculation of slight damage state for Bare frame - Model A.	40
A.3.1	PGA AND ISDR	43
A.3.2	Interpolation of OP, IO, DC, LS and CP damage state	43
A.3.3	Mean and Standard Deviation Calculation	44
A.3.4	Mean and Standard Deviation	44
A.3.5	Probability of exceedance calculation for Model C – PSW.	44

ABBREVIATIONS

RC	Reinforced Concrete
IS	Indian Standard
FEMA	Federal Emergency Management Agency
ATC	Applied Technology Council
FC	Fragility Curve
DCM	Displacement Coefficient Method
CSM	Capacity Spectrum Method
OP	Operational Level
IO	Immediate Occupancy
DC	Damage control
LS	Life Safety
CP	Collapse Prevention

CHAPTER 1

INTRODUCTION

1.1 General

India is a developing nation. The FSI (Floor Spacing Index) is increasing significantly in indian cities as a result of improved transportation and safety measures. People prefer to live in cities for economic reasons. As a result, metropolitan cities are feeling the need for more space to accommodate an expanding population. Because space is limited, structural engineers around the world are now being asked to design high-rise structures with stiffness anomalies in seismic zones.

The dynamic response of multistorey structural systems can be regulated. Improved material properties and more appropriate structural forms, such as masonry infill and shear walls, including solid and perforated shear walls.

Shear walls are essential components of buildings, particularly in regions prone to seismic activity. These vertical load-bearing elements provide structural stability by resisting lateral forces generated during earthquakes. Over the years, architectural trends have evolved, leading to the incorporation of perforations within shear walls for various reasons, such as aesthetics, functionality, and spatial requirements. However, this introduces a new dimension to structural design, requiring careful consideration of both seismic performance and fragility.

The seismic performance of buildings with shear walls is of utmost importance. During earthquakes, shear walls act as primary load-bearing elements, absorbing and dissipating seismic forces to protect the structural integrity of the building. By effectively

distributing these forces throughout the structure, shear walls reduce the risk of structural damage and collapse, safeguarding the occupants and contents within.

However, the presence of perforations within shear walls can affect their seismic performance and structural behavior. Perforations alter the stiffness and strength characteristics of the shear wall, potentially compromising its ability to resist lateral forces. Therefore, it is essential to carefully analyze and design shear walls with perforations to maintain the desired seismic performance.

Seismic fragility, on the other hand, refers to the vulnerability of a structure to seismic events. Shear walls without perforations typically exhibit higher resistance and lower fragility due to their solid and uninterrupted nature. In contrast, shear walls with perforations may introduce weak points or stress concentrations, potentially affecting their ability to withstand seismic loads. Thus, addressing the fragility of shear walls with perforations becomes a critical aspect of their design.

To optimize the seismic performance and mitigate fragility in buildings with shear walls and perforations, engineers employ advanced analysis techniques and design methodologies. These include considering factors such as the size, location, and shape of perforations, as well as the specific load conditions and seismic hazard levels. By employing performance-based design approaches and considering the dynamic response of the structure, engineers can ensure that shear walls with perforations maintain adequate strength, stiffness, and energy dissipation capacities during seismic events.

Furthermore, continuous research and advancements in seismic engineering contribute to the development of innovative construction techniques and materials, enabling the design of more resilient buildings with shear walls and perforations. Advanced modeling and simulation tools allow for accurate prediction of structural behavior and seismic response, facilitating the identification of critical areas and potential design improvements.

In conclusion, building with shear walls and shear walls with perforations are integral to modern structural design, particularly in seismic-prone regions. Shear walls provide enhanced seismic performance by resisting lateral forces, while perforations offer architectural versatility and functional benefits. However, the introduction of openings

must be carefully considered to maintain structural integrity and address fragility concerns. Through meticulous analysis, design, and consideration of seismic performance, engineers can optimize the behavior of shear walls with perforations, creating buildings that exhibit robustness, safety, and aesthetic appeal in the face of seismic events.

1.2 Seismic Fragility Curve

In the field of earthquake engineering, understanding the vulnerability of structures to seismic events is crucial for designing resilient and safe buildings. One powerful tool used for this purpose is the seismic fragility curve. The seismic fragility curve provides valuable insights into the likelihood of different levels of damage or failure for a given structure under varying levels of ground shaking.

A seismic fragility curve (FC) is a valuable tool used to assess the level of risk or safety associated with potential earthquake hazards. It provides a quantitative representation of the probability that a structure will experience a certain level of damage or exceed a specific performance threshold over time, considering a given earthquake hazard scenario. The FC is constructed by plotting the probability of exceeding a particular damage state against a seismic intensity parameter, such as peak ground acceleration (PGA) or peak spectral acceleration (Sa) or peak spectral displacement (Sd).

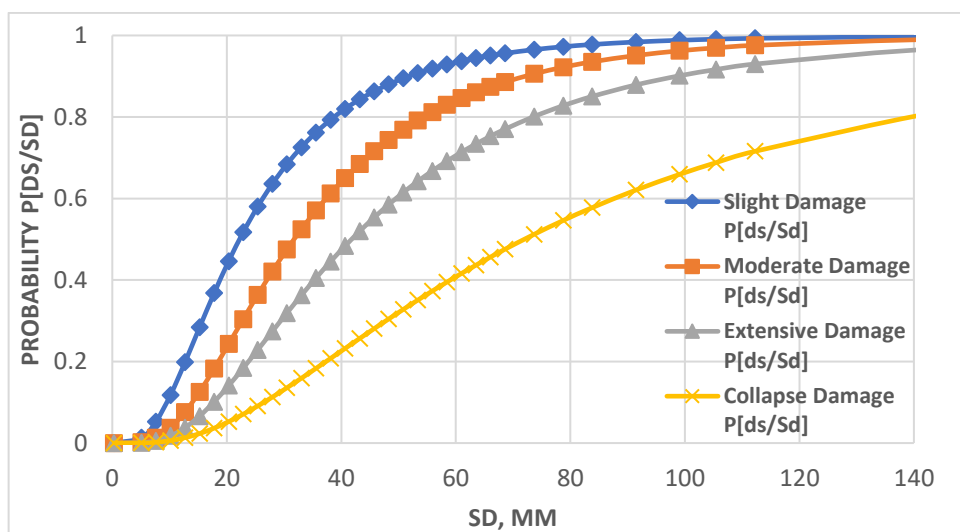


Fig. 1.1 Typical Fragility Curve.

Fragility curves provide valuable insights for seismic risk assessment, emergency planning, and building design. They aid in making informed decisions regarding risk mitigation, retrofitting strategies, and building code development. By analyzing the fragility curves, engineers can identify the vulnerability of different structural components, determine critical damage thresholds, and prioritize measures to enhance the resilience of structures against earthquakes.

It is important to recognize that fragility curves are specific to particular building types, structural systems, and geographical regions. Factors such as building height, configuration, material properties, and construction details must be considered when constructing and applying fragility curves. Therefore, it is crucial to use appropriate fragility curves tailored to the specific characteristics of the structure under evaluation.

To ensure accuracy, fragility curve development considers uncertainties associated with seismic hazard assessment, structural modeling, and ground motion variability. By incorporating these uncertainties, fragility curves provide a realistic estimation of structural vulnerability and enable informed decision-making in risk reduction strategies.

In conclusion, seismic fragility curves are powerful tools for evaluating the level of risk and safety associated with potential earthquake hazards. They quantify the probability of different damage states occurring given a certain seismic intensity. Fragility curves assist in risk assessment, emergency planning, and structural design, enabling stakeholders to prioritize resources and take appropriate measures to mitigate seismic risks. Ongoing advancements in data collection, analysis techniques, and modeling capabilities contribute to the continuous improvement and evolution of fragility curves, ultimately leading to the development of safer and more resilient structures in earthquake-prone regions.

1.3 Pushover Analysis Method

The displacement-based pushover analysis method is a widely used technique for assessing the structural behavior of buildings under lateral loads, particularly seismic forces. It involves incrementally applying lateral loads to the structure, starting from low

magnitudes and gradually increasing them until reaching a predefined performance limit or collapse condition. This method provides a simplified yet effective approach to capture the nonlinear response of structures, accounting for stiffness degradation and strength deterioration.

Two notable methods within the displacement-based pushover analysis are the Displacement Coefficient Method (DCM) and the Capacity Spectrum Method (CSM). The DCM, as outlined in FEMA-356, and the CSM, documented in ATC-40, both rely on nonlinear static analysis techniques to estimate the behavior of the structure.

The Capacity Spectrum Method visualizes the predicted seismic behavior of a structure by intersecting its capacity spectrum with the response spectrum, representing the earthquake's demands. The point of intersection, known as the performance point, provides an estimation of the displacement demand at a specific seismic hazard level.

On the other hand, the Displacement Coefficient Method utilizes a bilinear representation of the capacity curve and incorporates modification factors or coefficients to calculate a target displacement. The target displacement corresponds to a point on the capacity curve and is equivalent to the performance point in the capacity spectrum method.

It is important to acknowledge that while the displacement-based pushover analysis method provides valuable insights into the structural behavior and performance, it does have limitations. Simplified assumptions and approximations are made, introducing uncertainties in the analysis results. Careful consideration of lateral load patterns and the variability of ground motion characteristics is essential for accurate predictions.

In summary, the displacement-based pushover analysis method is a valuable tool for assessing the seismic behavior of structures. The DCM and CSM are two widely employed methods within this approach, providing engineers with insights into the displacement demand and overall performance of the structure. However, it is necessary to exercise engineering judgment and consider the limitations and uncertainties associated with this method.

1.4 Nonlinear time history analysis

Nonlinear time history analysis plays a significant role in the development of fragility curves for structural engineering applications. Fragility curves provide valuable information about the vulnerability of structures to different levels of ground motion or other dynamic loads. By incorporating nonlinear behavior into the analysis, the fragility curves can better capture the response of structures under extreme loading conditions. The advantage of using nonlinear time history analysis for fragility curve development is that it provides a more accurate representation of a structure's behavior. Nonlinearities, such as material and geometric nonlinearity, can significantly influence the response of structures. By accounting for these nonlinearities, the analysis can capture the actual structural performance more realistically, leading to more reliable fragility curves. This enables engineers to better understand the potential damage levels and failure modes of structures under different hazard scenarios.

However, there are also some disadvantages associated with nonlinear time history analysis in the context of fragility curve development. One of the main challenges is the computational complexity involved. Nonlinear analysis requires solving a system of nonlinear equations, which can be computationally demanding and time-consuming, especially for large-scale structures. This necessitates access to powerful computational resources and expertise in structural dynamics to ensure accurate and efficient analysis.

In summary, while nonlinear time history analysis is advantageous for fragility curve development due to its ability to capture the nonlinear behavior of structures, it also presents challenges in terms of computational complexity and the need for detailed modeling. Despite these drawbacks, the accuracy and realism provided by nonlinear analysis make it a valuable tool in developing robust fragility curves, ultimately enhancing the understanding of structural vulnerability to dynamic loads.

1.5 Objectives of the Study

Taking into account the aforementioned factors, the present study aims to accomplish the following primary goals:

- a) Analyze and compare the seismic performance of three building models: bare frame, shear wall, and perforated shear wall.
 - i. Evaluate the top storey displacement and storey drift of each building model under seismic loads.

- ii. Compare the lateral displacement and drift reduction achieved by each model in both X and Y directions.
- b) Develop fragility curves for each model, which can provide insights into their likelihood of damage or failure under different seismic events. Fragility curves will be created using two methods: the Nonlinear static pushover method and the Nonlinear Dynamics Time history method.
- c) The study will compare the performance of each building model at different damage states, such as slight, moderate, extensive, and collapse using the pushover method. Additionally, for the Nonlinear Dynamics Time history analysis, the performance will be evaluated at each damage state using the same performance levels (OP, IO, DC, LS, and CP).

By achieving these objectives, this research aims to contribute to the understanding of the seismic performance and develop fragility curves for different building models. This contribution will enhance the knowledge base and assist in the development of more resilient and safer building designs.

1.6 Organisation of the Thesis

Chapter 1: Introduction

The first chapter introduces the topic of the dissertation and provides an overview of the research. It emphasizes the importance of shear walls, including perforated shear walls, in providing structural stability and addressing space limitations. The research aims to optimize the seismic performance and mitigate fragility in buildings with shear walls and perforations through advanced analysis techniques and design methodologies. The displacement-based pushover analysis method is discussed as a valuable tool for evaluating structural behavior under lateral loads. The different performance levels of buildings in response to seismic forces are explained. And the objective of the present study.

Chapter 2: Literature Review

The second chapter presents a comprehensive literature review of previous research conducted on shear walls with or without perforations. It highlights key studies,

methodologies, and findings related to the behavior and performance of shear walls walls with or without perforations under seismic loads.

Chapter 3: Methodology

This chapter outlines the methodology employed in the study. It includes details of the parametric aspects of the model. The chapter provides a clear description of the research methodology followed to achieve the study objectives.

Chapter 4: Results and Discussions

Chapter 4 presents the results obtained from the analysis of four building models: bare frame, shear wall, and perforated shear wall. The findings are presented in the form of tables and graphs, allowing for a comprehensive interpretation and analysis of the results. The chapter includes detailed discussions on the significance and implications of the obtained results.

Chapter 5: Conclusions

The fifth chapter summarizes the key findings and conclusions drawn from the study. It provides a comprehensive overview of the outcomes obtained from the analysis and discusses their implications for future research. The chapter also highlights the scope for further investigation in the field.

Appendices

The appendices consist of three parts: First focuses on the calculation of the probability of exceedance, second provides pushover curves for different models and third focuses on the probability of exceedance calculation for time history results specifically for Model C-PSW.

References

The references section lists all the sources and studies cited throughout the dissertation. It ensures proper attribution and acknowledges the contributions of previous research in the field.

CHAPTER 2

LITERATURE REVIEW

2.1 General

To withstand earthquakes in high-risk areas, tall and high-rise buildings must meet a specific level of performance under earthquake loading (Astriana et al., 2017). Fragility curves have been developed by many researchers for different shear wall structures using various potential hazard parameters such as PGA, inter-story drift, and spectral displacement using HAZUS-MH MR4 or MR5 and ATC 40 manual. Generally, pushover and time history analysis are conducted to obtain the potential hazard parameters (Halder et al. 2016), (Kamath et al., 2017) and (Astriana et al., 2017).

2.2 Literature Review

Astriana et al., (2017) conducted a study to analyze the seismic performance of a moment resisting frame-shear wall system. They utilized seismic fragility curves to evaluate the system's behavior, taking into account potential hazard parameters such as Spectral displacement. The fragility curve was developed using information from HAZUS-MH MR5 and the ATC 40 manual. To compare the outcomes, the researchers presented the results from both sources in a graphical representation.

Nazari et al. (2017) employed time history analysis in PRFORM-3D software and applied incremental dynamic analysis (IDA) to develop fragility curves for two- and five-story buildings designed in accordance with the Canadian Building Code. The damage indicator was inter-storey drift of the first floor, while the seismic intensity parameter was spectral acceleration at the fundamental period.

Kamath et al., (2017) has developed the fragility curves for low-rise, mid-rise, and high-rise buildings using a HAZUS-MH MR4 technical manual by taking spectral displacement as the ground motion parameter.

Deb et al. (2016) conducted a study to develop fragility curves and investigate the impact of shear wall location on fragility for 2D reinforced concrete frames using SAP 2000 software. The damage criterion was determined based on the interstorey drift percentage, and seven different Peak Ground Acceleration (PGA) values were considered. MATLAB was utilized to synthesize 30 ground motions for each PGA value, and the target spectrum was derived from IS 1893:2002 for medium type soil.

Halder et al. (2016) evaluate the seismic vulnerability of a low-rise RC frame building using non-linear static analysis with SAP2000 to find the capacity curve of the building. They develop fragility curves for different damage grades based on HAZUS methodology and find that the building may experience moderate to severe damage states for different seismic hazard levels.

Sharma et al., (2015) discusses the importance of rigidity and stability in tall buildings to resist lateral forces. Shear walls contribute to lateral stiffness and strength, but regular openings decrease stiffness. The study examines the effects of different sizes and shapes of openings in shear walls on 30-story buildings. The provision of openings in shear walls reduces stiffness, leading to increased displacement and inter-story drift. Incorporating adjacent boundary elements helps increase stiffness and decrease displacement and inter-story drift. However, openings in shear walls introduce high local stress concentrations around the corners.

Saruddin et al. (2015) developed fragility curves for low- and mid-rise buildings in Malaysia, which included three- and six-story frame structures designed based on Eurocodes. The study utilized incremental dynamic analysis (IDA) with SAP2000 software. To assess the structural performance, the study considered five levels of performance-based seismic designs: operational phase, immediate occupancy, damage control, life safety, and collapse prevention.

Muthukumar et al., (2014) study focused on the behavior of shear walls with openings in seismic areas. It was found that the size and location of openings significantly affect the behavior of shear walls. Nonlinear finite element analysis was used to investigate the dynamic behavior of shear walls under various opening locations. A large number of small openings resulted in better displacement response, and strengthening was important for slender shear walls with staggered openings. The shear wall with four windows was considered the best for both slender and squat shear walls.

Marius et al., (2013) investigates the failure mechanisms of RC structural walls with staggered openings, which have been found to exhibit high rigidity, bearing capacity, and ductility during seismic events. Factors that influence their failure include the shape and sizes of the walls and openings, reinforcement and opening layout, site conditions, earthquake type, and strain rates. The study involved theoretical and experimental analysis to compare the sequence of yielding of reinforcement and crushing of concrete. The study's main objectives are to present the recorded failure mechanisms after earthquakes, explain their modes, and analyze the benefits of staggered openings in reinforced concrete structural walls under seismic loads.

Sakurai et al., (2012) conducted an analysis employing non-linear finite element methods was employed to examine the shear force contributions and stress transfer mechanisms in RC shear walls containing openings. To assess the shear strength of these walls, a simplified model for shear resistance was proposed. Notably, it was observed that the tension in boundary columns accounted for a relatively small portion, approximately 10% or less, of the maximum shear strength. The developed model also accounts for the impact of varying influential parameters on the shear strength of reinforced concrete shear walls with multiple openings.

Mieses et al. (2007) conducted research on a multistory residential structure with shear walls in Puerto Rico. The study utilized the time history method to analyze the building's structure and evaluate its damage based on the inter-story drift ratio. The fragility curves were developed as a function of PGA for various damage states, including minor, moderate, substantial, and major.

Wu et al., (2003) study used non-linear finite element analysis to examine the behavior of walls with irregular openings under earthquake loading. The results showed that flanges and axial load increased load carrying capacity but decreased ductility, while smaller openings positioned away from the boundary could help maintain strength, stiffness, and ductility. The study suggests that strengthening walls along the load paths could improve their performance.

CHAPTER 3

METHODOLOGY

3.1 Problem Statement

The study conducted on a G+10-story RCC structure with complex geometry, which is modeled in ETABS software. The building is located in a high seismic zone IV with a medium soil site condition. The concrete used in the building has a grade of 25 MPa, and the reinforcement bars have a grade of Fe 500.

The foundation of the frame is considered to be fixed. In this study: bare frame, shear wall frame, and perforated shear wall frame structure has been taken. Slab is represented as a thin shell. The parapet wall is set at a height of 1 meter. It is important to note that the main goal of this study is to assess the seismic performance and vulnerability of shear walls in structures with and without perforations. The results of this study can contribute to the development of safer and more resilient structures in high seismic zones.

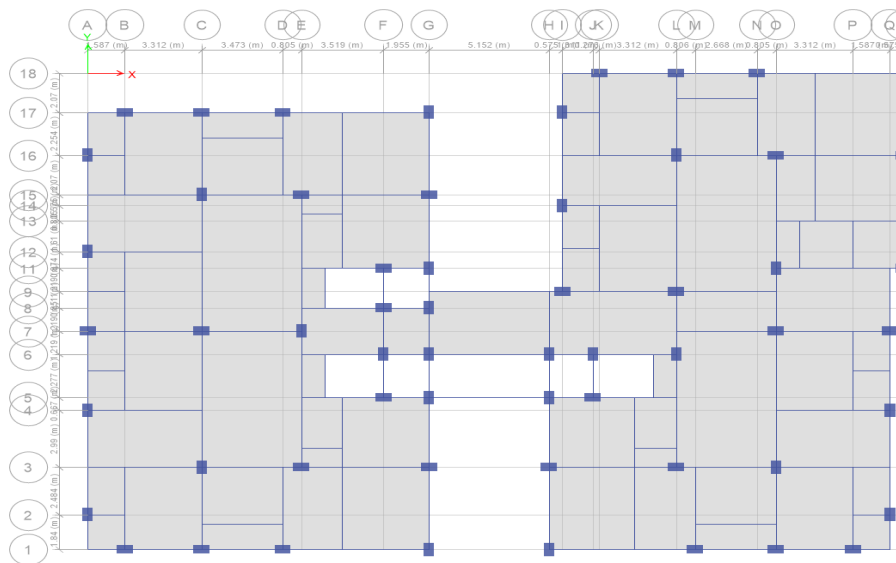


Fig.3.1 Building plan (Source: Vaibhav Keshari [1])

Table 3.1 Building Description

Particulars	Dimension/Size/Value
Number of stories	G+10
Height of floor and ground floor	3m
Slab Depth	150mm
Beam Size	300X450mm ²
Column Size	500X700mm ²

Table 3.2 Load Description

Loading	Intensity
Live load on each floor	3 kN/mm ²
Floor finish	1 kN/mm ²
Roof load	1.5 kN/mm ²
Parapet load	3kN/m

Model-A. Bare frame structure

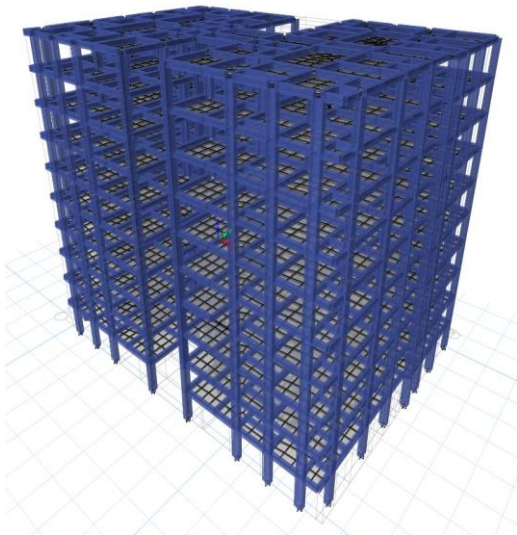


Fig.3.2 Model A- Bare frame structure

Model-B. Shear wall framed structure

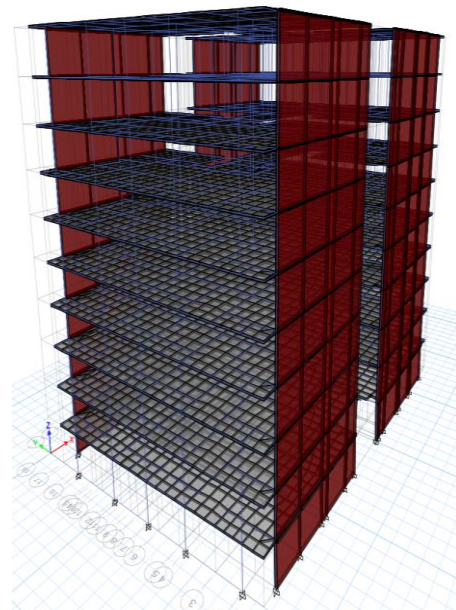


Fig.3.3 Model B- Shear wall framed structure

Model-C. Perforated shear wall frame structure

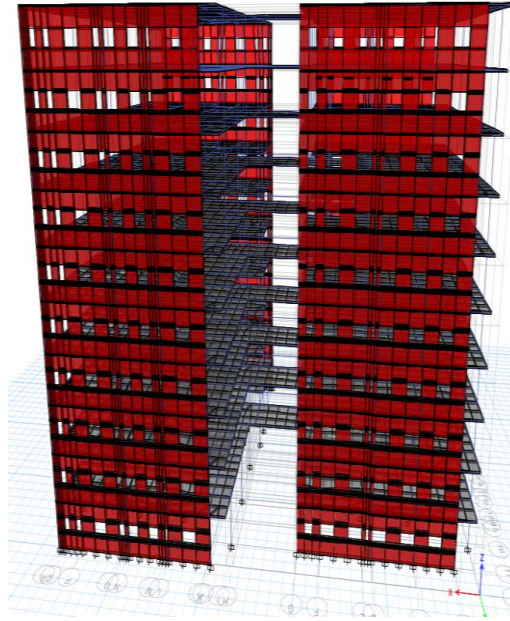


Fig.3.4 Model C- Perforated shear wall frame structure

After modeling the structure as per Table 3.1 in ETABS software, different types of loads depicted in Table 3.2 such as dead, live, floor finishes, roof, and parapet loads were applied. The data obtained from the analysis, including lateral displacement and drift for all three models, were plotted on graphs for further analysis.

3.2 Construction of pushover curves.

Pushover analysis is a method used to subject a structure to a lateral load pattern that continuously increases through elastic and inelastic behavior until an ultimate condition is reached. This static nonlinear approach is commonly used to evaluate a structure's response to seismic events. To analyze the nonlinear behavior of the structure, default hinges were assigned to the structural elements in accordance with ASCE 41-13. A load combination of $DL+0.25*LL$ was used as a predecessor to the pushover case in both the X and Y directions. The analysis produces a capacity curve that represents the relationship between base shear and roof displacement. This curve can be used to determine various parameters, such as displacement at yield and ultimate, which are important for structural evaluation and seismic risk assessment.

For this study, displacement-based pushover analysis was performed using ETABS. The capacity curve was obtained from the display menu of ETABS, showing the structure's response to lateral loading. The capacity curve was then transformed into a bilinear capacity spectrum, and the values of displacement at yield (D_y) and ultimate displacement (D_u) were computed. These values were further converted into spectral displacement at yield spectral displacement (S_{dy}) and ultimate spectral displacement (S_{du}), respectively. Following the guidelines of HAZUS 5.1 [2], fragility curves were developed using these values to assess the structure's vulnerability to seismic events.

3.3 Development of fragility curves.

3.3.1 Development of fragility curves by pushover method.

The literature has seen several studies on fragility curve evaluation of structures; however, no specific approach is available. To develop fragility curves, the guidelines from the HAZUS 5.1 [2] technical manual have been adopted. The HAZUS methodology was formulated for FEMA to mitigate seismic hazards in the United States. The technical manual provides the procedure for deriving fragility curves. As per HAZUS 5.1 [2], The model used for determining the probability of being in or surpassing a specific damage state employs a cumulative lognormal distribution. In the context of structural damage, the likelihood of being in or surpassing a particular damage state, given the spectral displacement (S_d), is represented as follows:

$$P[d_s/S_d] = \Phi [1/\beta_{d_s} * \ln (S_d/ S_{d,d_s})] \quad (3.1)$$

Here, S_{d,d_s} represents the median value of spectral displacement at which the building reaches the damage state threshold, d_s . β_{d_s} denotes the standard deviation of the natural logarithm of spectral displacement for the damage state, d_s . Φ represents the standard normal cumulative distribution function.

Table 3.3 HAZUS Damage state thresholds

Damage State	Median Spectral Displacement ($S_{d,ds}$)
Slight	$S_{d,S} = 0.7 * S_{d,y}$
Moderate	$S_{d,M} = S_{d,y}$
Extensive	$S_{d,E} = S_{d,y} + 0.25(S_{d,u} + S_{d,y})$
Complete	$S_{d,C} = S_{d,u}$

Where, $S_{d,y}$ and $S_{d,u}$ are the spectral displacement at yield and ultimate.

The β_{ds} value can be directly taken from the tables given in HAZUS technical manual.

Table 3.4 S_{sd} and βS_{ds} assumed as per HAZUS Manual.

	Model A		Model B and C	
Damage state	S_{sd}, in	β_{ds}, in	S_{sd}, in	β_{ds}, in
Slight	2.16	0.66	1.73	0.68
Moderate	4.32	0.64	4.32	0.65
Extensive	12.96	0.67	12.96	0.66
Complete	34.56	0.78	34.56	0.76

3.3.2 Development of fragility curves by time history method.

To assess the performance of the proposed structure under lateral loads, the drifts will be measured to identify critical damage levels that could potentially lead to structural collapse. The percentage drift (% drift) can be calculated by dividing the maximum roof displacement by the total height of the building, as shown in Equation (3.2):

$$\% \text{ Drift} = (\text{Roof displacement} / \text{Building height}) * 100 \quad (3.2)$$

Several seismic parameters play a role in developing fragility curves. In this study, the Peak Ground Acceleration (PGA) parameter was used in the Incremental Dynamic Analysis (IDA) and is also utilized for developing vulnerability curves. The performance levels that define the damage states for the three models are as follows: OP, IO, DC, LS, and CP.

To develop the fragility curves, two main parameters are required: the mean (μ) and standard deviation (σ). Equations has been used for developing fragility curves.

$$P[Ds/PGA] = \Phi((\ln (PGA) - \mu)/\sigma) \quad (3.3)$$

where Φ represents the standard normal cumulative distribution function, μ and σ are the mean value and standard deviation of the logarithm of PGA, respectively, and Ds represents the damage state.

By applying these calculations and equations, the fragility curves can be developed, providing valuable insights into the likelihood of different damage.

CHAPTER 4

RESULTS AND DISCUSSIONS

4.1 Results

The study aims to assess seismic performance of the bare frame and shear walls with and without perforations. To achieve this objective, several parameters, including lateral displacement and drift in both X and Y directions, were analyzed for three structural models: Model A - Bare frame structure, Model B - Shear wall framed structure and Model C - Perforated shear wall frame structure. The results were plotted in a graph to compare and evaluate the influence of shear walls on the structural behavior. The graph also depicts the damage sustained by the structural elements of both models during the seismic event.

Table 4.1 Lateral Displacement (mm) along X Direction. (Push X Results)

Story	Elevation (m)	Model-A	Model-B	Model-C
Base	0	0	0	0
Story1	3	36.597	1.035	1.193
Story2	6	86.386	2.562	2.869
Story3	9	136.828	4.397	4.83
Story4	12	183.199	6.458	6.993
Story5	15	223.657	8.659	9.274
Story6	18	257.51	10.933	11.606
Story7	21	284.688	13.225	13.935
Story8	24	305.434	15.491	16.217
Story9	27	320.308	17.703	18.425
Story10	30	330.558	19.836	20.532

Table 4.2 Lateral Displacement (mm) along Y Direction. (Push X Results)

Story	Elevation (m)	Model-A	Model-B	Model-C
Base	0	0	0	0
Story1	3	0.774	0.098	0.078
Story2	6	1.781	0.247	0.165
Story3	9	2.892	0.426	0.241
Story4	12	3.917	0.625	0.306
Story5	15	4.833	0.837	0.358
Story6	18	5.687	1.054	0.4
Story7	21	6.458	1.27	0.434
Story8	24	7.106	1.483	0.501
Story9	27	7.533	1.689	0.577
Story10	30	7.761	1.89	0.682

Table 4.3 Story Drifts along X Direction. (Push X Results)

Story	Elevation (m)	Model-A	Model-B	Model-C
Base	0	0	0	0
Story1	3	0.012199	0.000345	0.000398
Story2	6	0.016596	0.000509	0.000558
Story3	9	0.016814	0.000611	0.000654
Story4	12	0.015457	0.000687	0.000721
Story5	15	0.013486	0.000733	0.000762
Story6	18	0.011284	0.000758	0.000778
Story7	21	0.009059	0.000764	0.000777
Story8	24	0.006915	0.000755	0.000761
Story9	27	0.004958	0.000737	0.000736
Story10	30	0.003417	0.000711	0.000703

Table 4.4 Story Drifts along Y Direction. (Push X Results)

Story	Elevation (m)	Model-A	Model-B	Model-C
Base	0	0	0	0
Story1	3	0.000258	0.000033	0.000026
Story2	6	0.000346	0.00005	0.000029
Story3	9	0.00037	0.00006	0.000025
Story4	12	0.000342	0.000066	0.000023
Story5	15	0.000305	0.000071	0.000024
Story6	18	0.000284	0.000072	0.000025
Story7	21	0.000257	0.000072	0.000025
Story8	24	0.000216	0.000071	0.000025
Story9	27	0.000142	0.000069	0.000025
Story10	30	0.000076	0.000067	0.000025

Table 4.5 Lateral Displacement (mm) along X Direction. (Push Y Results)

Story	Elevation (m)	Model A	Model-B	Model-C
Base	0	0	0	0
Story1	3	1.242	0.056	0.289
Story2	6	2.548	0.091	0.144
Story3	9	3.729	0.19	0.249
Story4	12	4.778	0.348	0.44
Story5	15	5.688	0.532	0.658
Story6	18	6.441	0.734	0.894
Story7	21	7.046	0.95	1.142
Story8	24	7.706	1.173	1.396
Story9	27	8.214	1.398	1.65
Story10	30	8.607	1.629	1.909

Table 4.6 Lateral Displacement (mm) along Y Direction. (Push Y Results)

Story	Elevation (m)	Model-A	Model-B	Model-C
Base	0	0	0	0
Story1	3	45.177	39.891	41.757
Story2	6	101.491	105.316	109.103
Story3	9	157.15	173.416	178.519
Story4	12	207.813	236.752	242.722
Story5	15	251.591	292.164	298.725
Story6	18	287.72	338.286	345.244
Story7	21	316.11	374.698	381.9
Story8	24	337.363	401.663	408.982
Story9	27	351.984	420.164	427.49
Story10	30	361.517	432.262	439.527

Table 4.7 Story Drifts along X Direction. (Push Y Results)

Story	Elevation (m)	Model-A	Model-B	Model-C
Base	0	0	0	0
Story1	3	0.000006	0.000019	0.000004
Story2	6	0.000014	0.000026	0.000004
Story3	9	0.000018	0.000041	0.000005
Story4	12	0.000021	0.000052	0.000007
Story5	15	0.000023	0.000061	0.000008
Story6	18	0.000022	0.000068	0.000009
Story7	21	0.000017	0.000072	0.000011
Story8	24	0.000013	0.000074	0.000011
Story9	27	0.000021	0.000075	0.000012
Story10	30	0.000033	0.000077	0.000013

Table 4.8 Story Drifts along Y Direction. (Push Y Results)

Story	Elevation (m)	Model-A	Model-B	Model-C
Base	0	0	0	0
Story1	3	0.017688	0.013297	0.013919
Story2	6	0.021775	0.021828	0.022483
Story3	9	0.021405	0.022711	0.023145
Story4	12	0.019427	0.021112	0.021401
Story5	15	0.016797	0.018471	0.018668
Story6	18	0.013901	0.015374	0.015506
Story7	21	0.01096	0.012137	0.012219
Story8	24	0.008131	0.008989	0.009027
Story9	27	0.005588	0.006167	0.00617
Story10	30	0.003626	0.004033	0.004013

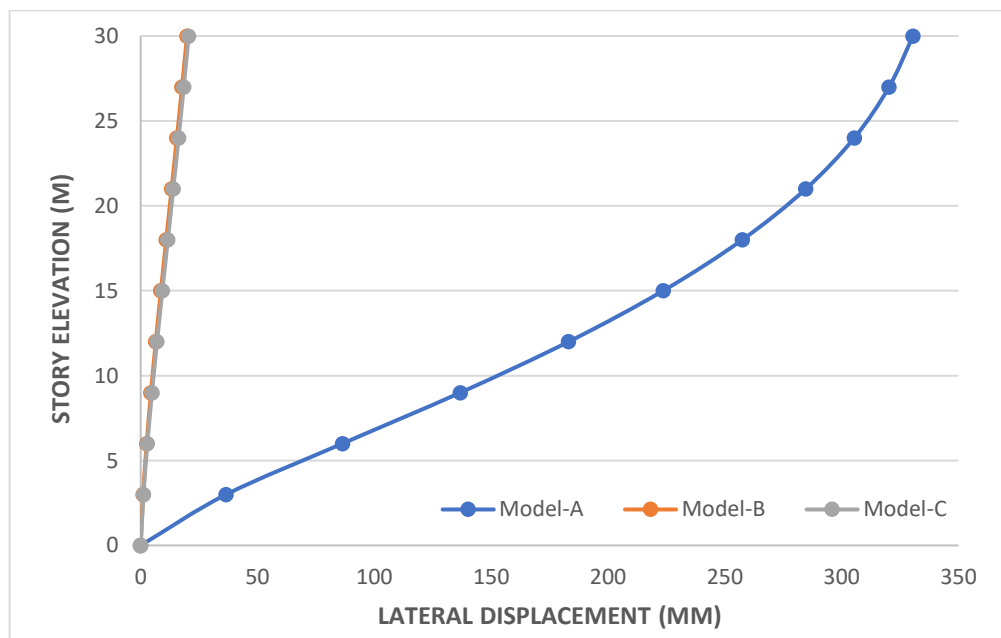


Fig. 4.1 Lateral Displacement (mm) along X Direction for Push X Case.

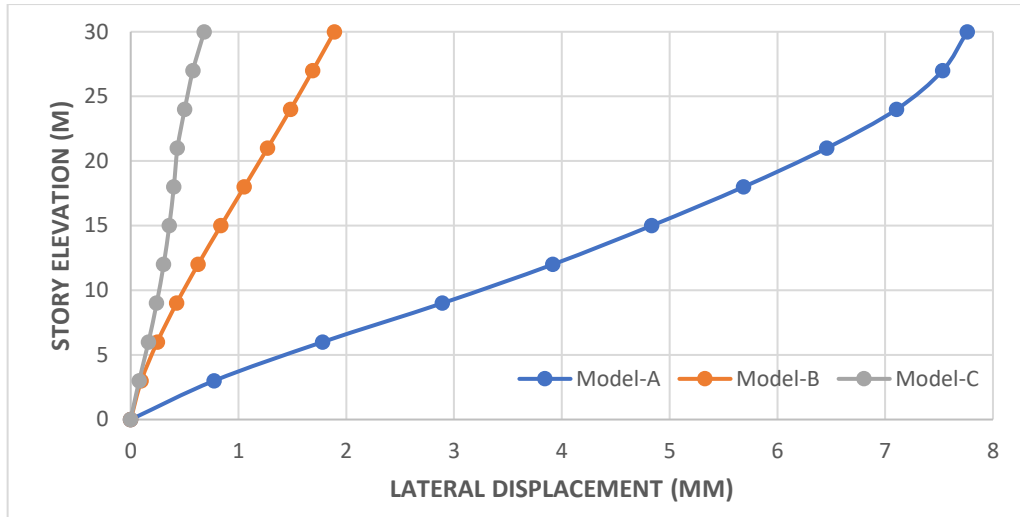


Fig. 4.2 Lateral Displacement (mm) along Y Direction for Push X Case.

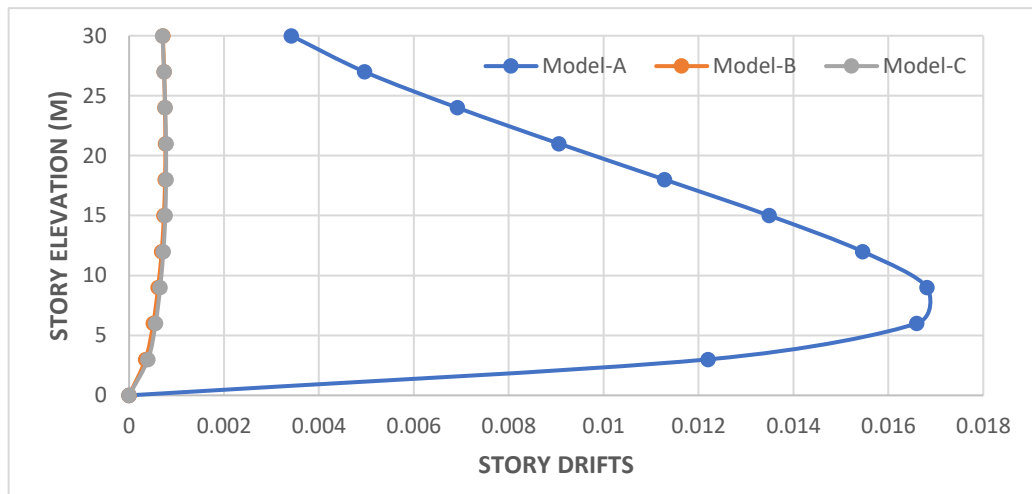


Fig. 4.3 Story Drifts along X Direction for Push X Results.

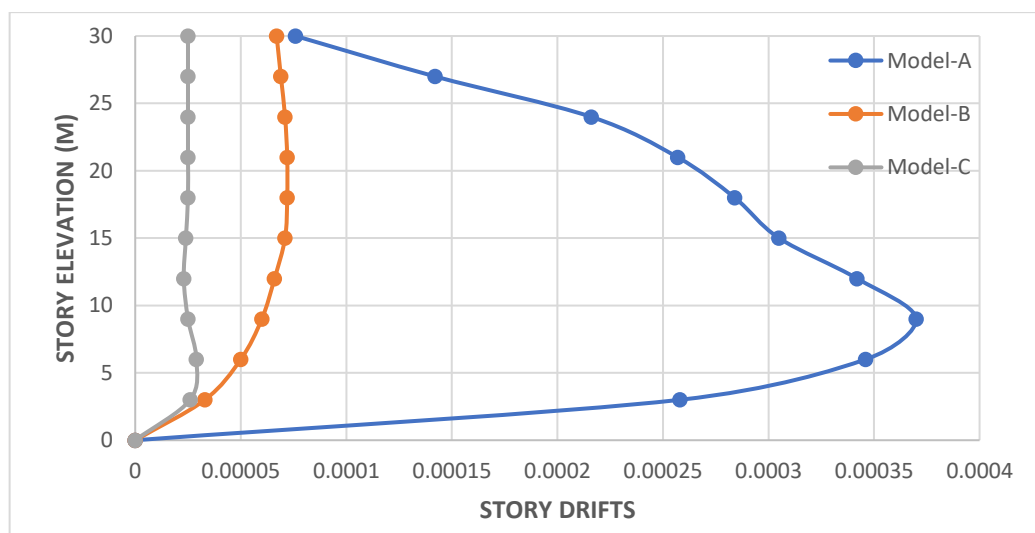


Fig. 4.4 Story Drifts along Y Direction for Push X Results.

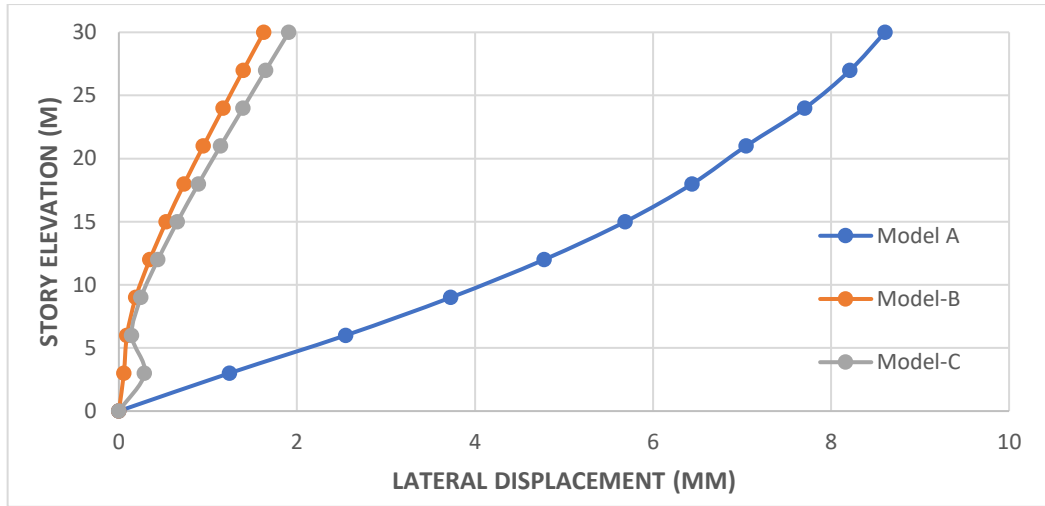


Fig. 4.5 Lateral Displacement (mm) along X Direction for Push Y Case.

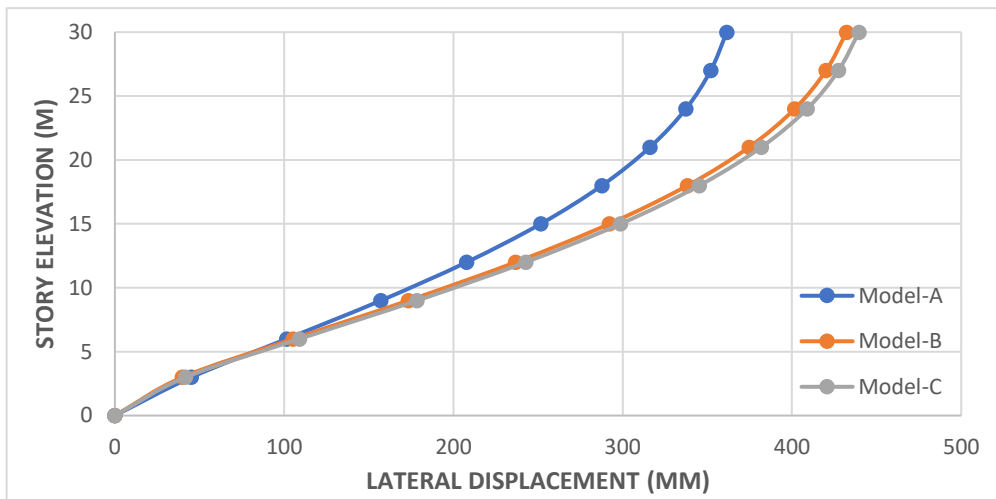


Fig. 4.6 Lateral Displacement (mm) along Y Direction for Push Y Case.

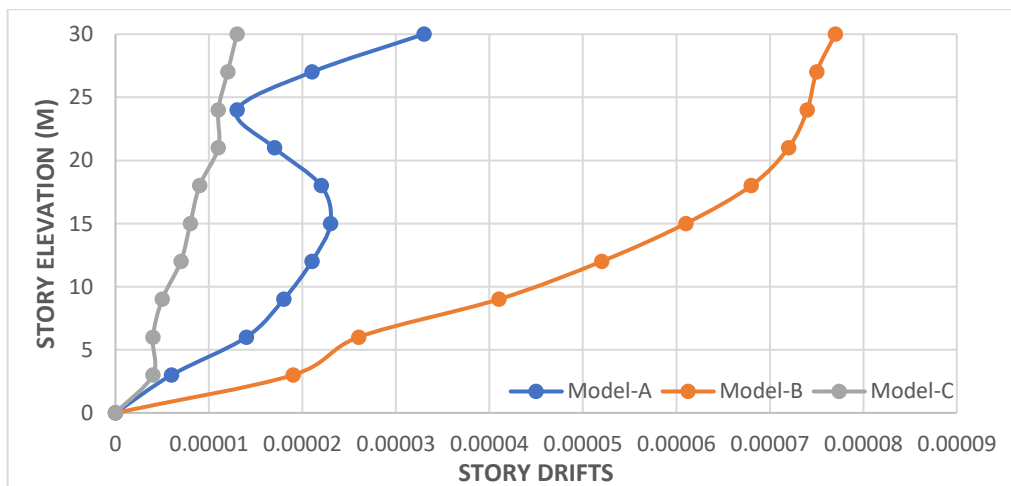


Fig. 4.7 Story Drifts along X Direction for Push Y Results.

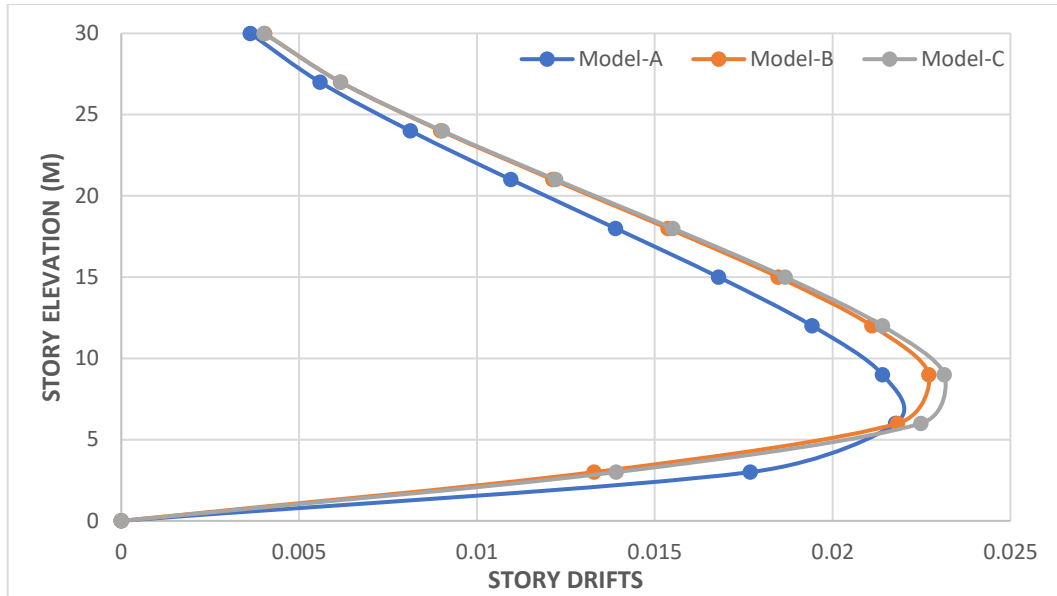


Fig. 4.8 Story Drifts along Y Direction for Push Y Results.

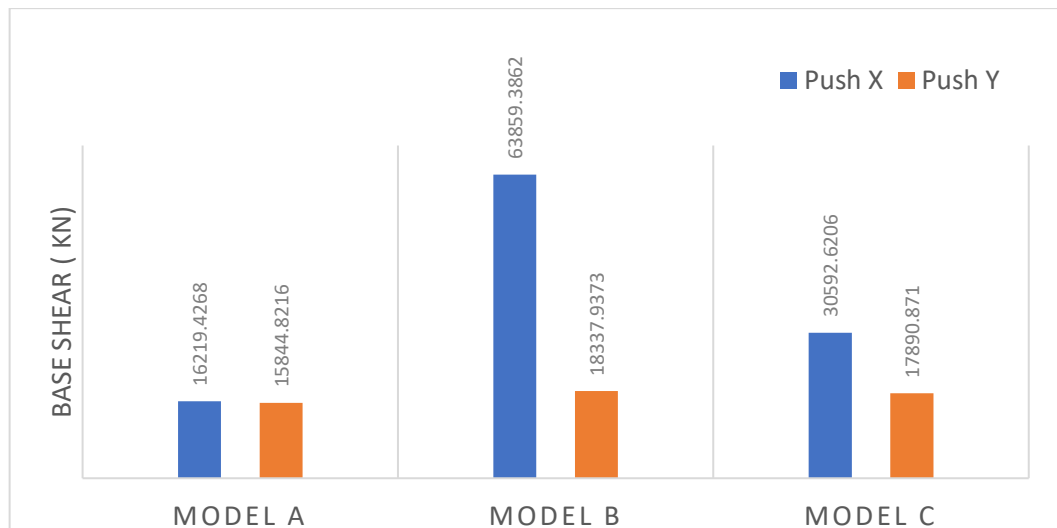


Fig. 4.9 Base shear for different models.

4.2 Discussions

The following observations were observed from the above analysis:

A. Comparison of results of Model B: Shear wall frame structure with Model A: Bare Frame

Pushover X cases:

1. The top floor lateral displacement in Model B was reduced by 94% and 75.6% compared to the base model - Model A in the X and Y directions. Additionally, the drift at the top floor level in Model B was reduced by 79.2% and 11.8% compared to the base model in the X and Y directions.
2. In the X and Y directions during the pushover X case, the lateral displacement in Model B was reduced by 97.17% and 87.34% both at the first floor compared to the base model. Similarly, the drift in Model B was reduced by 97.17% and 87.21% both at first floor as compared to base model (Model A).

Pushover Y cases:

3. In the pushover Y case, Model B exhibited an 81% reduction in lateral displacement at the top floor level compared to the base model (Model A), with an increase of 19.5% in the X and Y directions. Additionally, the drift at the top floor level in Model B was significantly increased by 133% and 11.2% in the X and Y directions, respectively, compared to the base model (Model A).
4. In the X and Y directions during the pushover Y case, the lateral displacement in Model B was reduced by 96.43% at the second floor and 11.7% at the first floor as compared to the base model. Similarly, the drift in Model B was increased by 469.23% at eighth floor and reduced 24.83% at first floor as compared to base model (Model A).

B. Comparison of results of Model C: Perforated shear wall frame structure with Model A: Bare Frame

Pushover X cases:

5. The top floor lateral displacement in Model C was reduced by 93.7% and 91.21% compared to the base model - Model A in the X and Y directions. Additionally, the

drift at the top floor level in Model C was reduced by 79.42% and 67.10% compared to the base model in the X and Y directions.

6. In the X and Y directions during the pushover X case, the lateral displacement in Model C was reduced by 96.74% at the first floor and 93.28% at the seventh floor respectively as compared to the base model (Model A). Similarly, the drift in Model C was reduced by 96.73% at first floor and 93.27% at fourth floor respectively as compared to the base model (Model A).

Pushover Y cases:

7. In the pushover Y case, Model C exhibited an 77.82% reduction in lateral displacement at the top floor level compared to the base model (Model A), with an increase of 21.57% in the X and Y directions. Additionally, the drift at the top floor level in Model C exhibited an 60.60% reduction in lateral displacement at the top floor level compared to the base model (Model A), with an increase of 10.67% in the X and Y directions.
8. In the X and Y directions during the pushover Y case, the lateral displacement in Model C was reduced by 94.34% at the second floor and 7.57% at the first floor respectively as compared to the base model (Model A). Similarly, the drift in Model C was reduced by 72.22% at third floor and 21.30% at the first floor respectively as compared to the base model (Model A).

C. Comparison of results of Model C: Perforated shear wall frame structure with Model B: Shear wall frame structure

Pushover X cases:

9. The top floor level lateral displacement in Model C was found to be 3.50% higher than the Model B, with a reduction of 63.91% in the X and Y directions during the pushover X case. Similarly, the drift at the top floor level in Model C was reduced by 1.1% and 62.6% compared to the Model B in the X and Y directions during the pushover X case.

10. The lateral displacement in Model C was found to be 15.26% higher than the Model B at the first floor, with a reduction of 66.21% at the eighth floor in the X and Y directions respectively during the pushover X case. Additionally, the drift of Model C was found to be 15.36% higher than the Model B at the first floor, with a reduction of 66.19% at the fifth floor in the X and Y directions respectively.

Pushover Y cases:

11. The top floor level lateral displacement in Model C was higher by 17.18% and 1.6% compared to the Model B in the X and Y directions during the pushover Y case. Similarly, the drift at the top floor level in Model C was reduced by 83.1% and 0.5% compared to the Model B in the X and Y directions during the pushover Y case.
12. In the pushover Y case, the lateral displacement in Model C was higher by 416.07% and 4.67% compared to the Model B in the X and Y directions. Furthermore, the drift in Model C was reduced by 87.80% at the third floor and 4.67% at the first floor compared to the Model B in the X and Y directions.
13. Both Model B and C exhibited similar behavior in the X direction for both pushover cases, as indicated by the overlapping curves on the graph.

D. Comparison of results of Base Shear

The base shear for Model A remains relatively consistent across different pushover cases. However, when analyzing Model B using pushover analysis in the X direction, it is observed that the base shear is higher compared to both Model A and Model C.

4.3 Construction of Fragility Curves

This study focuses on developing fragility curves for three building models. Fragility curves are used to determine the likelihood of different levels of damage based on the building's response to peak seismic forces and its capacity.

Model-A. Bare Frame

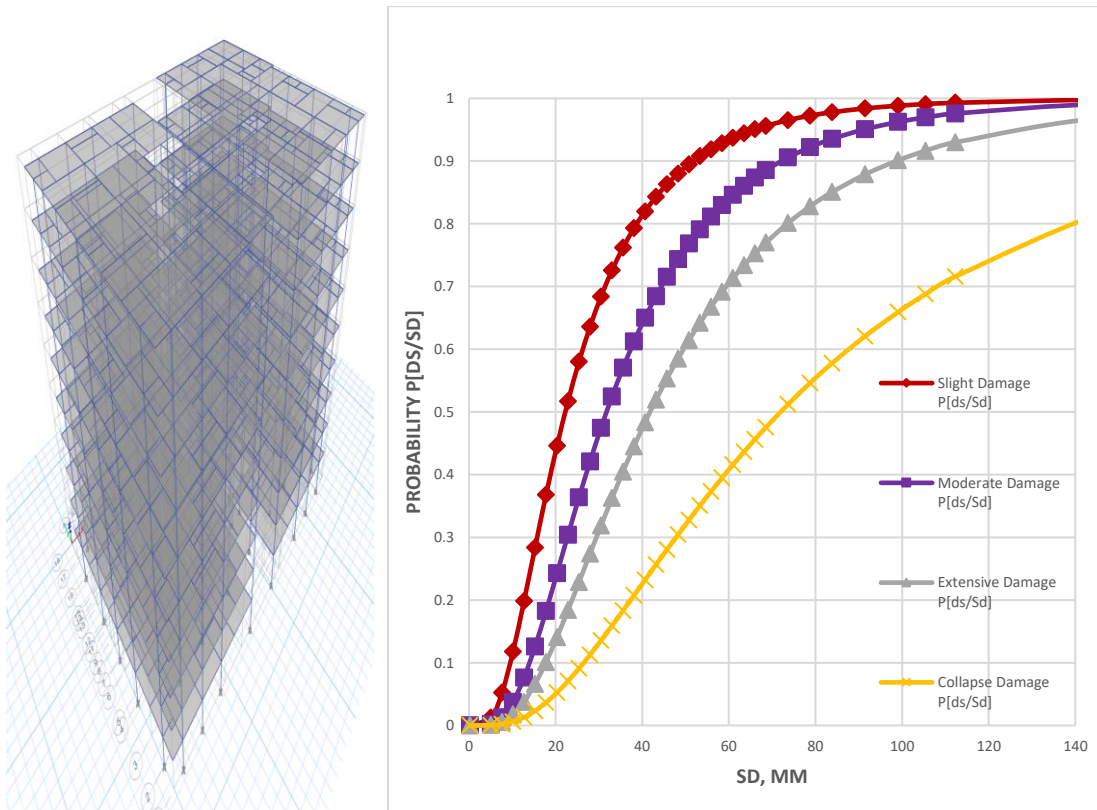


Fig. 4.10 Model A- Bare Frame.

Fig. 4.11 Fragility curve for bare frame by pushover analysis.

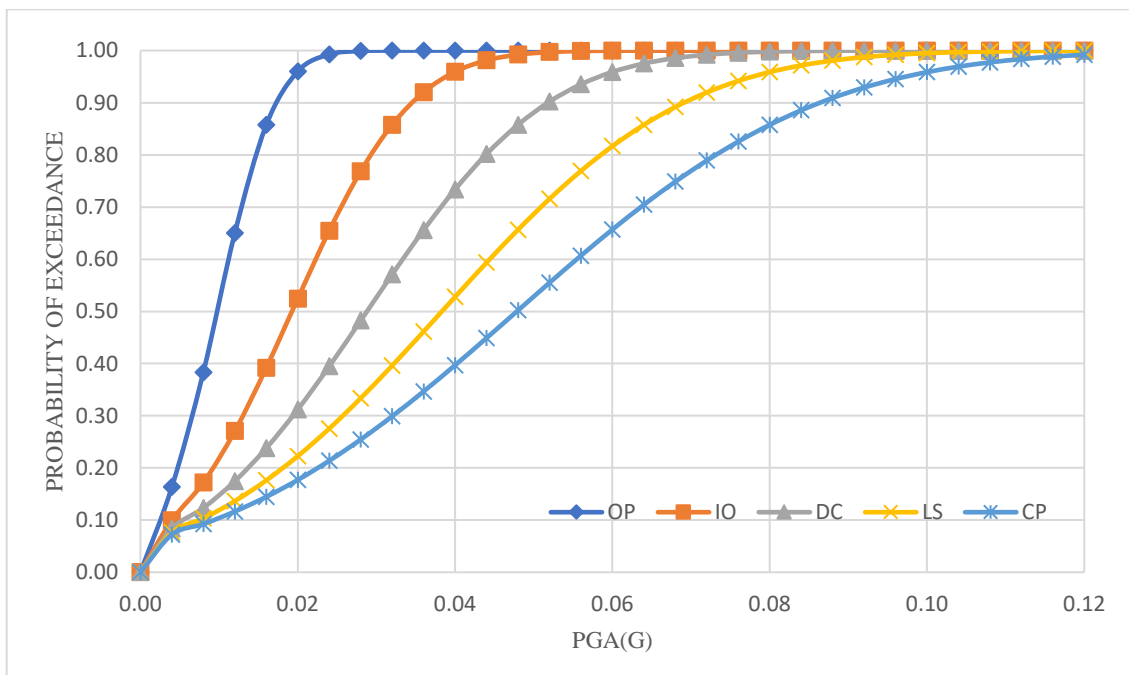


Fig. 4.12 Fragility curve for bare frame by time history method.

Model-B. Shear wall structure.

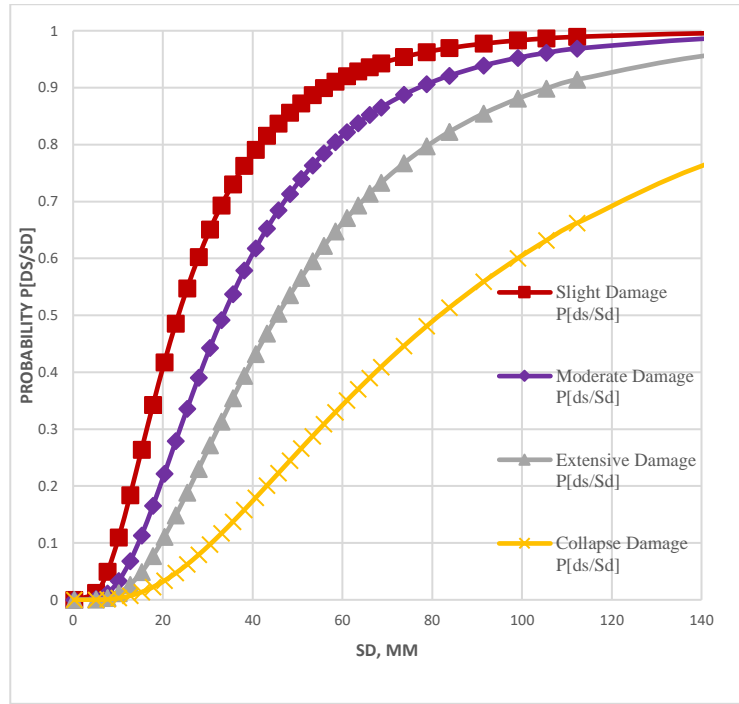
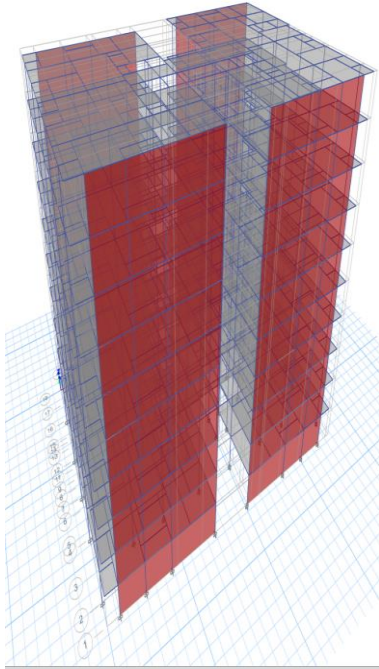


Fig. 4.13 Model B- Shear wall structure.

Fig. 4.14 Fragility curve for shear wall structure by pushover analysis.

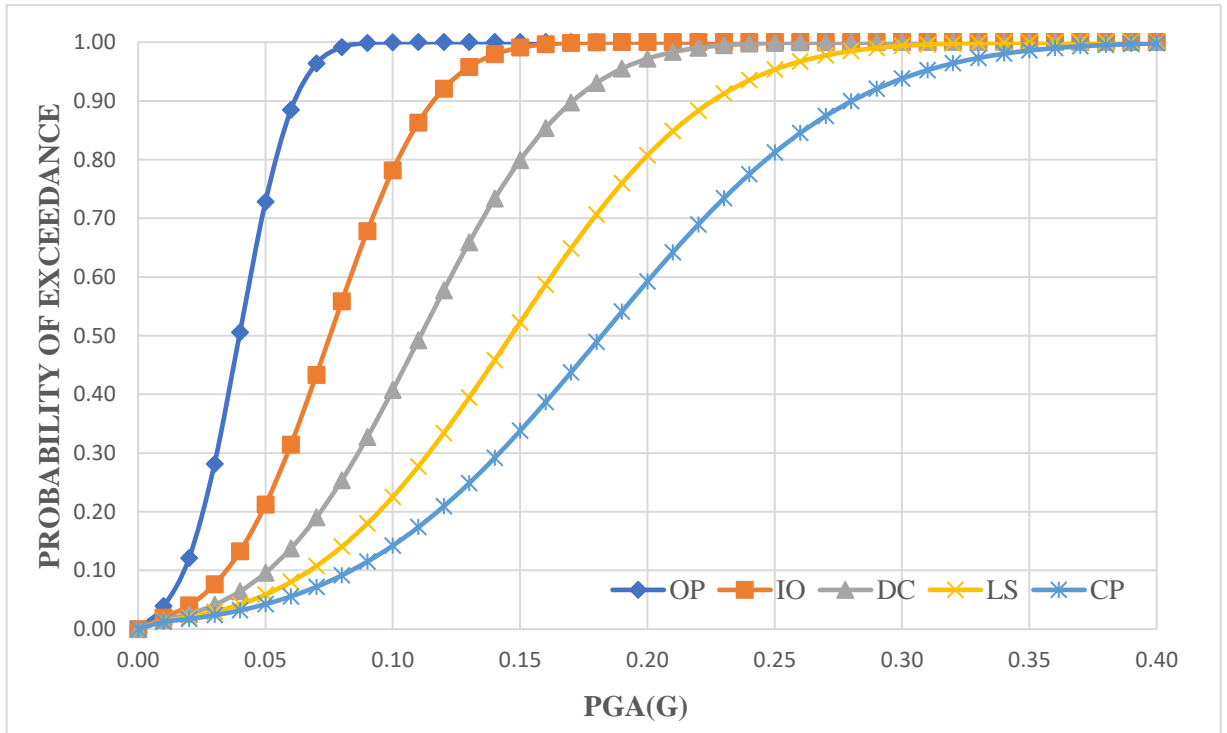


Fig. 4.15 Fragility Curve for shear wall structure by time history method.

Model-B. Perforated Shear wall structure

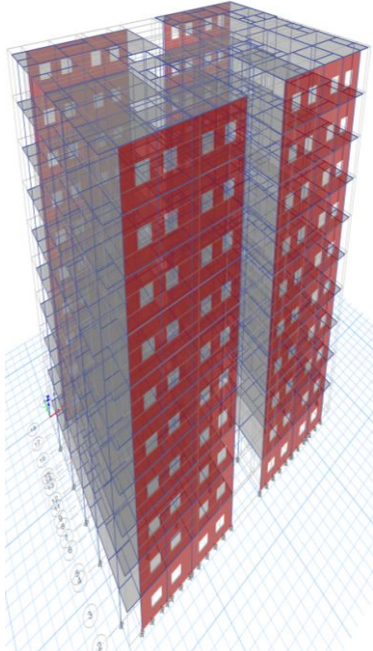


Fig. 4.16 Model B- Perforated Shear wall structure.

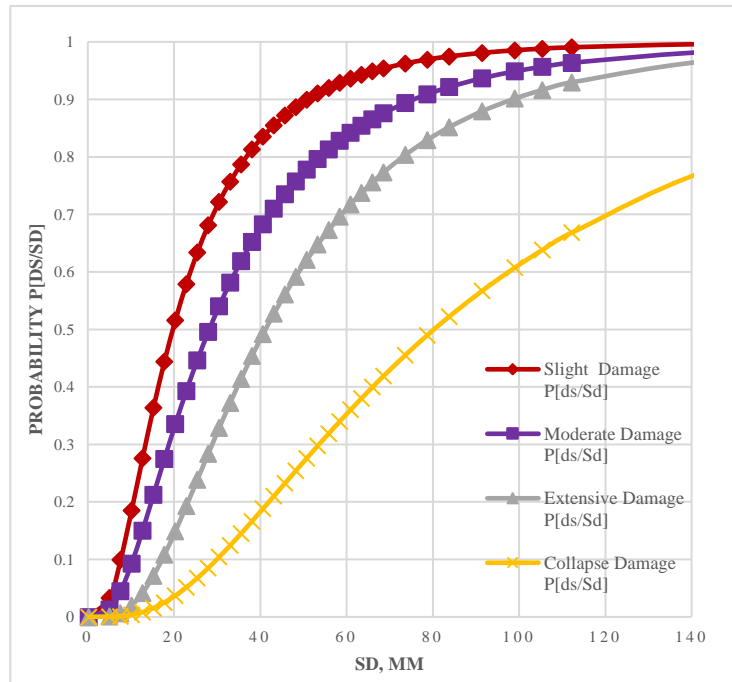


Fig. 4.17 Fragility Curve for Perforated Shear wall by pushover analysis.

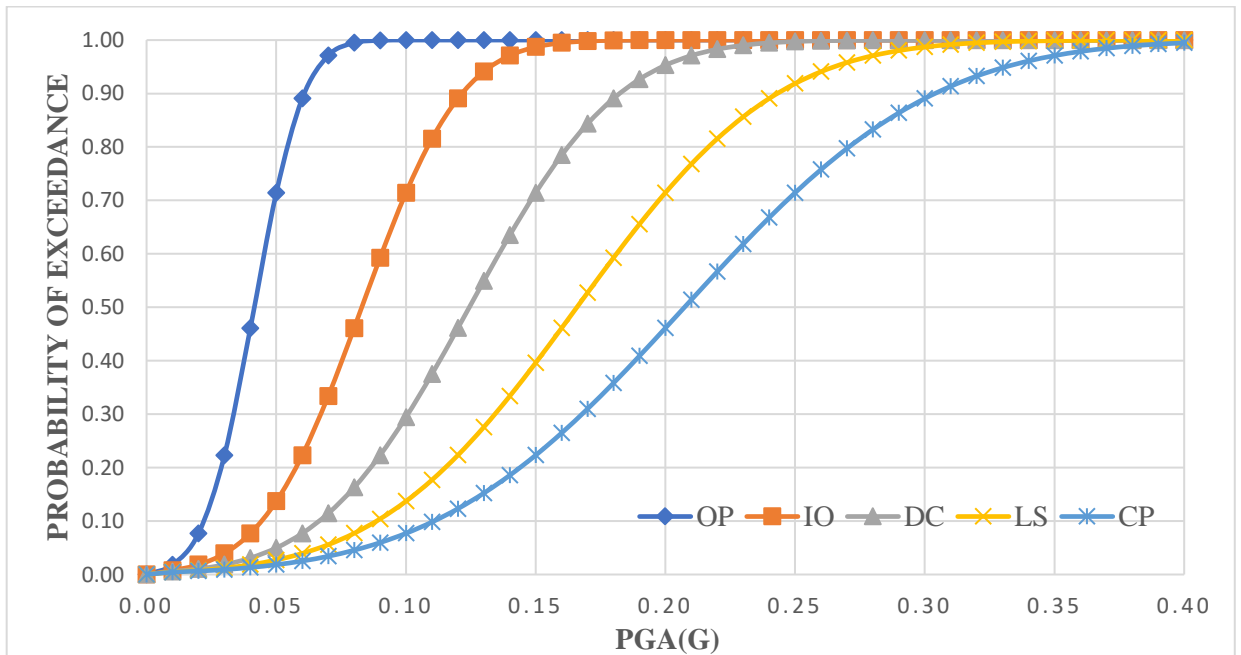


Fig. 4.18 Fragility curve for perforated shear wall time history method.

4.4 Comparison of fragility of different damage state by pushover analysis results.

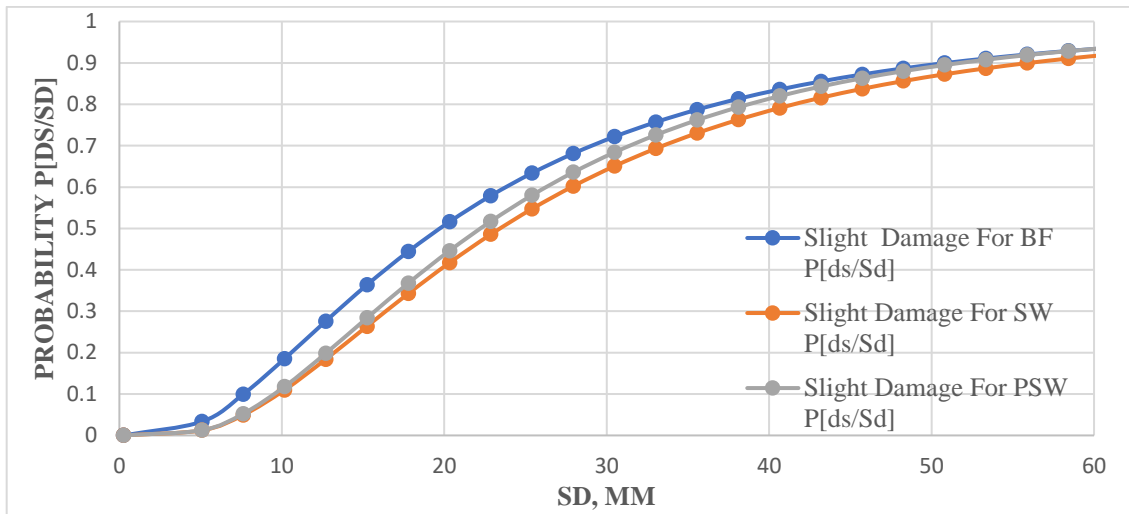


Fig. 4.19 Fragility Curve for Slight Damage for BF, SW and PSW.

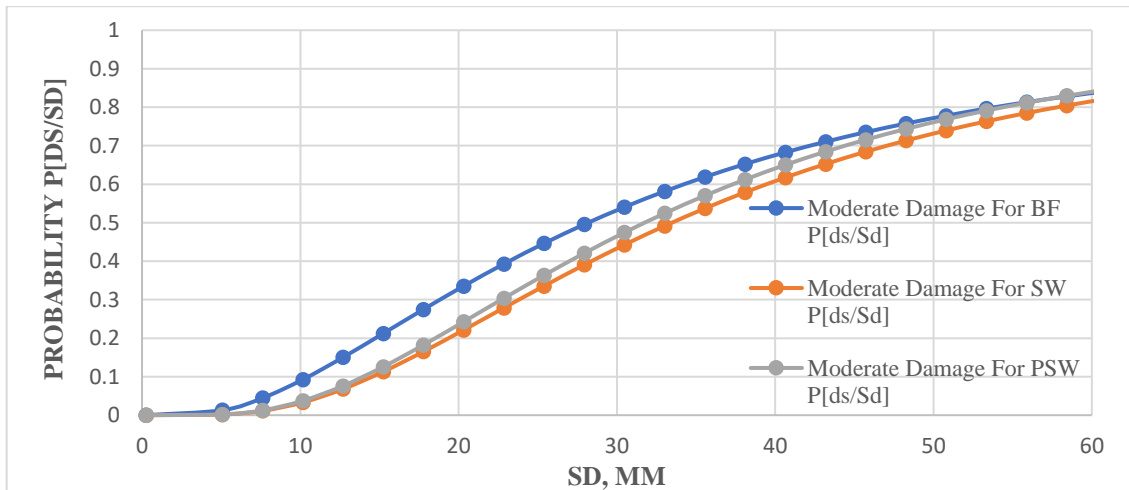


Fig. 4.20 Fragility Curve for Moderate Damage for BF, SW and PSW.

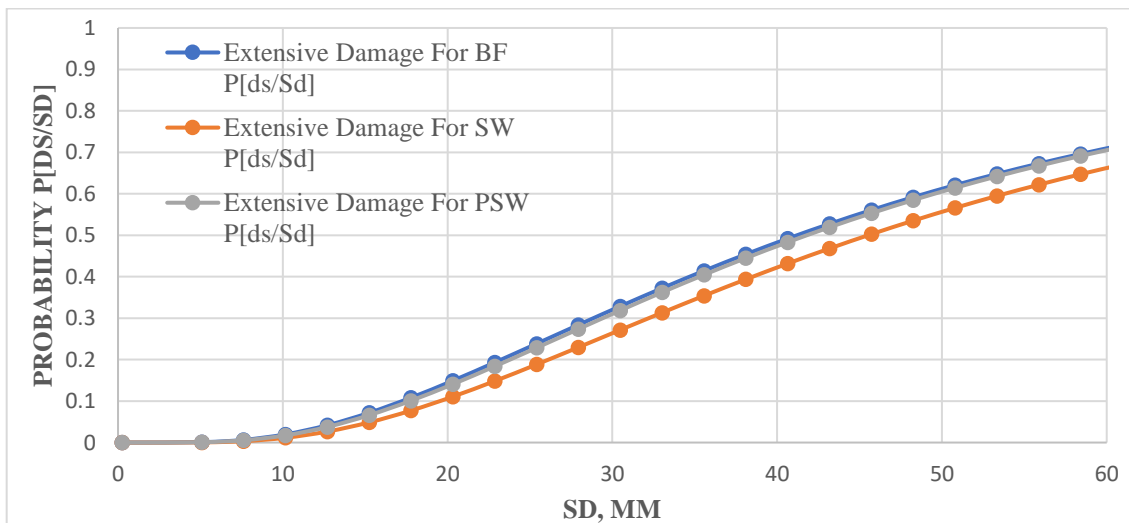


Fig. 4.21 Fragility Curve for Extensive Damage for BF, SW and PSW.

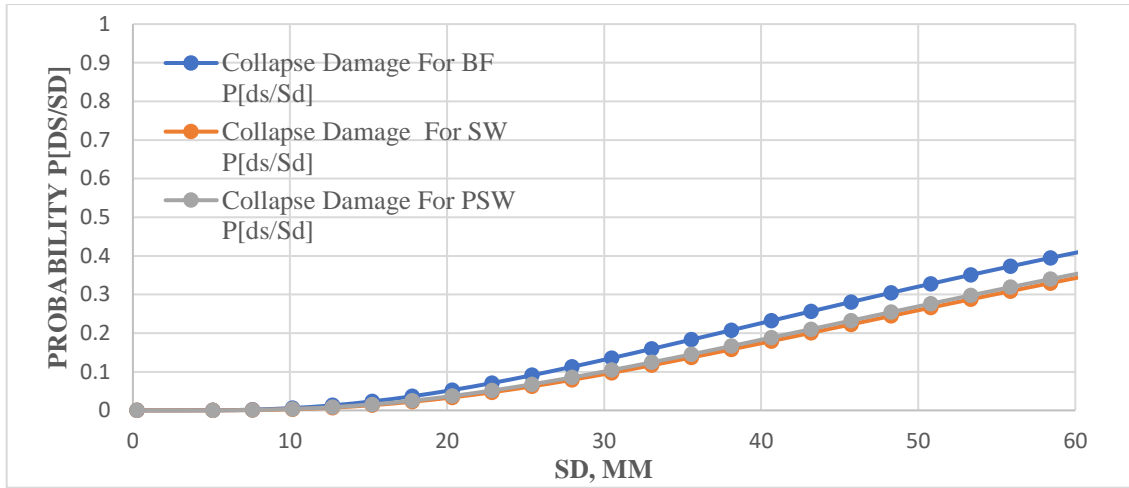


Fig. 4.22 Fragility Curve for Collapse Damage for BF, SW and PSW.

4.5 Comparison of fragility of different damage state by time history analysis results.

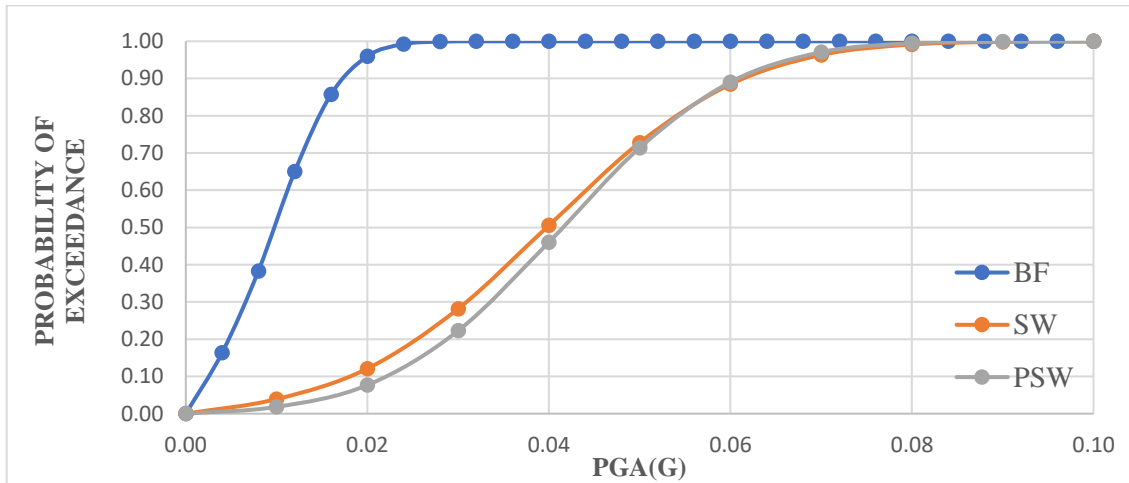


Fig. 4.23 Fragility Curve of OP for BF, SW and PSW.

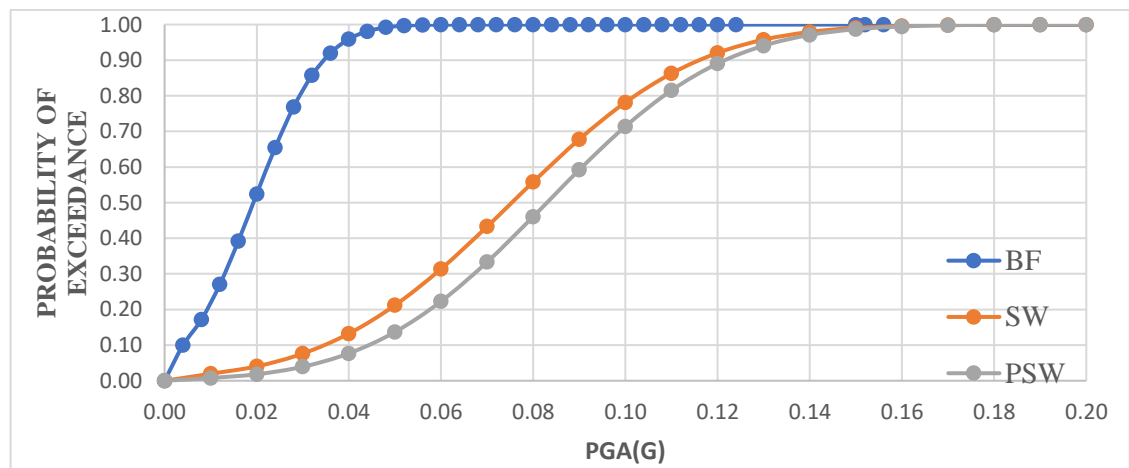


Fig. 4.24 Fragility Curve of IO for BF, SW and PSW.

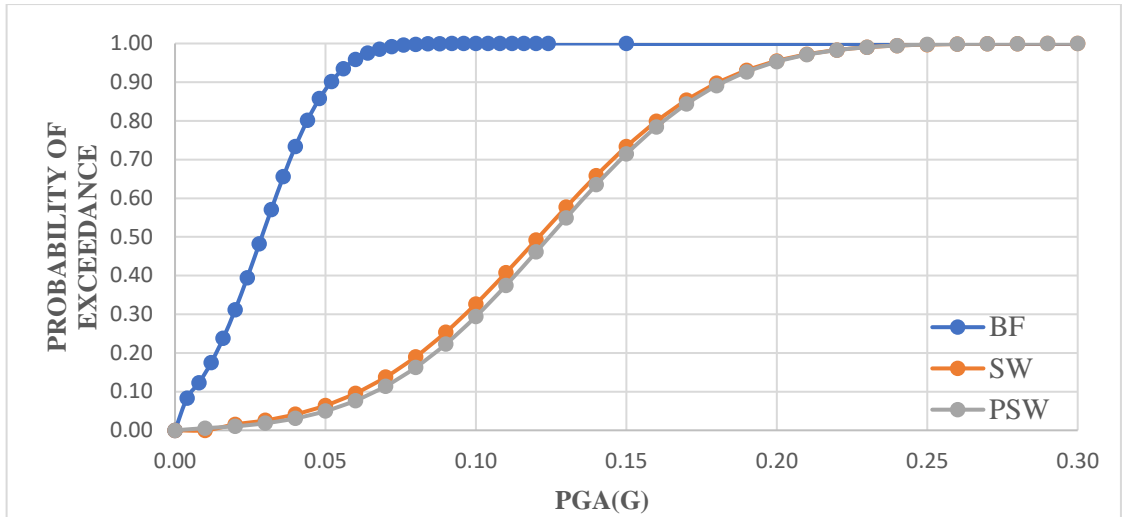


Fig. 4.25 Fragility Curve of DC for BF, SW and PSW.

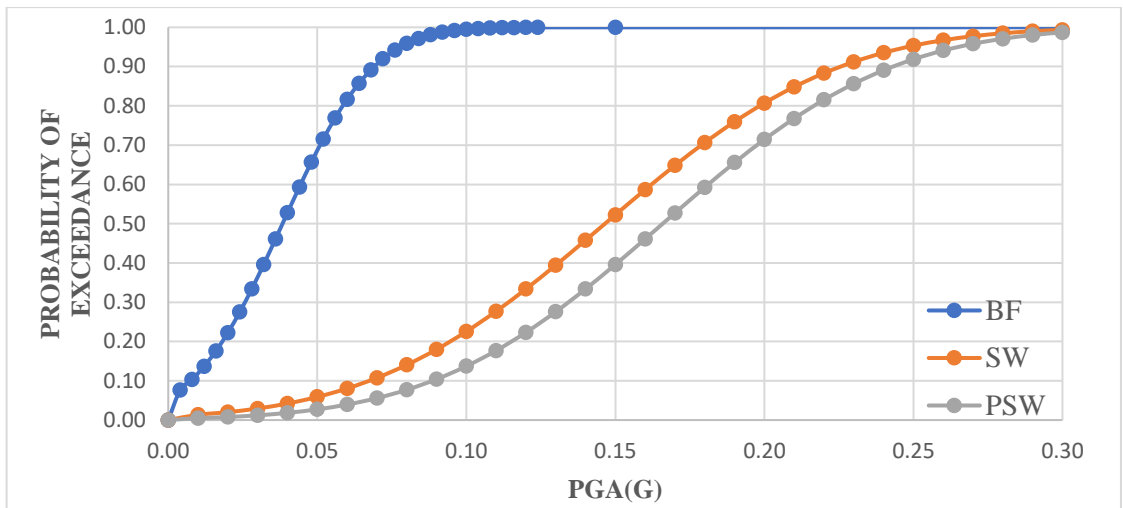


Fig. 4.26 Fragility Curve of LS for BF, SW and PSW.

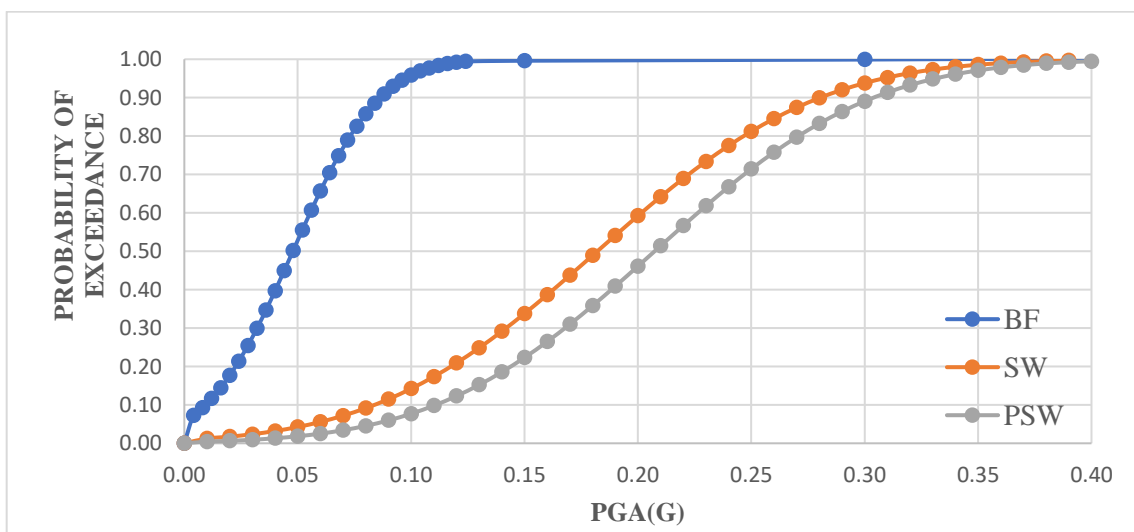


Fig. 4.27 Fragility Curve of CP for BF, SW and PSW.

CHAPTER 5

CONCLUSION

5.1 Conclusion

In conclusion, based on the analysis conducted:

- I. Model B (Shear wall frame structure) showed significant improvements compared to the base model (Model A - Bare Frame) in terms of reducing lateral displacement and drift in both pushover X and Y cases.
- II. Model C (Perforated shear wall frame structure) also demonstrated notable enhancements compared to the base model (Model A) with substantial reductions in lateral displacement and drift.
- III. When comparing Model C with Model B, Model B generally outperformed Model C, achieving lower lateral displacements and greater drift reductions.
- IV. However, in the pushover Y case, Model C exhibited higher lateral displacements compared to Model B, although it still achieved reduced drift values at certain floor levels.
- V. Both Model B and Model C exhibited similar behavior in the X direction for both pushover cases, suggesting comparable performance in that regard.
- VI. The choice between Model B and Model C would depend on specific project requirements and priorities, considering factors such as lateral displacement, drift reduction, and structural design considerations.
- VII. These findings highlight the effectiveness of shear wall frame structures (Model B and Model C) in enhancing seismic performance when compared to the bare frame structure (Model A).

- VIII. The pushover analysis in the X direction reveals that Model B exhibits a higher base shear compared to both Model A and Model C, while the base shear remains consistent for Model A across different pushover cases.
- IX. The inclusion of shear walls in a frame structure has a notable impact on its seismic behavior, effectively improving both its strength and lateral stiffness.
- X. Additionally, the study suggests that extending shear walls throughout the entire height of a building is unnecessary, as their effectiveness decreases in the upper storeys due to reduced lateral stiffness. This insight can potentially lead to cost savings in construction.
- XI. Fig. no.4.19 to 4.22 illustrates a significant trend: Model A exhibits a higher vulnerability compared to Model C, and Model C displays a higher vulnerability compared to Model B, particularly in the slight, moderate, extensive, and collapse damage states.
- XII. Fig. no.4.23 to 4.27 illustrates a significant trend: Model A exhibits a higher vulnerability compared to Model B, and Model B displays a higher vulnerability compared to Model C, particularly in the OP, IO, DC, LS and CP damage states.

In summary, the results of the analysis indicate that incorporating shear wall frame structures (Model B and Model C) can significantly improve the seismic performance and fragility of buildings compared to a bare frame structure (Model A). Model B generally showed better performance compared to Model C, achieving lower lateral displacements and greater drift reductions. However, the choice between the two models should be based on specific project requirements and considerations.

5.2 Scope of Future Work

In future research, it is recommended to explore the following aspects:

- a) Conduct an additional study to assess the influence of factors such as the size of the opening, percentage of opening, and building height at various locations. This investigation will provide deeper insights into the behavior and performance of shear walls with or without perforations under different configurations.
- b) Utilize software programs such as STAAD Pro, SAP, ANSYS, Midas Gen, and other relevant applications in addition to ETABS. This broader implementation of software tools will expand the scope of analysis and allow for validation of the research findings.
- c) Extend the analysis methods beyond pushover analysis to incorporate linear static, linear dynamic (response spectrum technique), P- Δ non-linear analyses, modal analysis, and non-linear time history analyses for the same building models. This comprehensive approach will provide a more accurate understanding of the structural response under various loading conditions.

By addressing these aspects, the research can advance the understanding of the seismic performance of buildings with shear walls and perforations. This knowledge will contribute to the development of more resilient and safer building designs in the future.

APPENDICES

Appendix 1: Probability of exceedance calculation for pushover results.

To generate fragility curves, the following steps were taken:

- a) Displacement-based pushover analysis was performed using ETABS software.
- b) The pushover curves were obtained from the display menu of ETABS, as shown in Appendix 2, and the corresponding displacement values were recorded in Table A.1.1.

Table A.1.1 Values for different parameters.

	Model A	Model B	Model C
Vy (kN)	9033.745	9329.179	7957.366
Ki (kN/m)	71082.24	75428.4	75440.18
Dy (mm)	127.08	125.27	105.47
Du (mm)	288.082	305.479	300.507
Sdy (mm)	31.75	33.47	28.18
Sdu (mm)	71.95	81.68	80.287
MPF	0.017948	0.020107	0.019909
MDF (mm)	0.223	0.186	0.188

- c) The pushover curve was transformed into a bilinear capacity spectrum according to ASCE 41-13 NSP using ETABS. The displacement values at yield (Dy) and ultimate displacement (Du) were then computed.

where, Dy was calculated as the ratio of base shear at yield (Vy) to the initial stiffness at yield (Ki).

Du was obtained from the target displacement taken from the pushover curve.

- d) These displacement values were then converted into spectral displacement at yield (Sdy) and ultimate spectral displacement (Sdu) using the following equations:

$$Sdy = \frac{Dy}{MPF * MDF} \quad (A.1.1)$$

$$S_{du} = \frac{D_u}{MPF * MDF} \quad (A.1.2)$$

where D_y represents the roof displacement at yield, D_u represents the roof displacement at ultimate, MPF is the first mode participation factor, and MDF is the first mode modal displacement roof.

- e) HAZUS damage thresholds for each model were calculated using Table 3.3.
- f) The probability of exceeding each damage state was determined by referencing Equation 3.1. The calculations are presented in Table A.1.2, utilizing the corresponding β_{ds} values from Table 3.4.
- g) Following the guidelines of HAZUS 5.1 [2], fragility curves were developed by plotting the S_d values on the X-axis and the corresponding normal distribution values on the Y-axis.

Table A.1.2 Probability of exceedance calculation of slight damage state for Bare frame - Model A.

Sd, inch	ln (Sd)	Ss,d, inch	ln (Sd/Ss,ds)	ln (Sd/Ss,ds)	1/β _{ds} *ln (Sd/Ss, ds)	Norm.S. Dist	Sd, mm
						P[ds/Sd]	
0.01	-4.60517	0.874998	-0.13353	-4.47164	-6.77521	6.21E-12	0.254
0.2	-1.60944	0.874998	-0.13353	-1.4759	-2.23622	0.012669	5.08
0.3	-1.20397	0.874998	-0.13353	-1.07044	-1.62188	0.052415	7.62
0.4	-0.91629	0.874998	-0.13353	-0.78276	-1.186	0.117812	10.16
0.5	-0.69315	0.874998	-0.13353	-0.55961	-0.8479	0.198247	12.7
0.6	-0.51083	0.874998	-0.13353	-0.37729	-0.57165	0.283778	15.24
0.7	-0.35667	0.874998	-0.13353	-0.22314	-0.33809	0.367646	17.78
0.8	-0.22314	0.874998	-0.13353	-0.08961	-0.13577	0.446	20.32
0.9	-0.10536	0.874998	-0.13353	0.028173	0.042686	0.517024	22.86
1	0	0.874998	-0.13353	0.133533	0.202323	0.580168	25.4
1.1	0.09531	0.874998	-0.13353	0.228844	0.346733	0.635604	27.94
1.2	0.182322	0.874998	-0.13353	0.315855	0.478568	0.683877	30.48
1.3	0.262364	0.874998	-0.13353	0.395898	0.599845	0.725695	33.02
1.4	0.336472	0.874998	-0.13353	0.470006	0.71213	0.761808	35.56
1.5	0.405465	0.874998	-0.13353	0.538999	0.816664	0.79294	38.1
1.6	0.470004	0.874998	-0.13353	0.603537	0.91445	0.81976	40.64
1.7	0.530628	0.874998	-0.13353	0.664162	1.006306	0.842866	43.18
1.8	0.587787	0.874998	-0.13353	0.72132	1.092909	0.862783	45.72
1.9	0.641854	0.874998	-0.13353	0.775387	1.174829	0.879968	48.26
2	0.693147	0.874998	-0.13353	0.826681	1.252546	0.894815	50.8
2.1	0.741937	0.874998	-0.13353	0.875471	1.326471	0.907658	53.34
2.2	0.788457	0.874998	-0.13353	0.921991	1.396956	0.918787	55.88
2.3	0.832909	0.874998	-0.13353	0.966443	1.464307	0.928445	58.42

2.4	0.875469	0.874998	-0.13353	1.009002	1.528791	0.936842	60.96
2.5	0.916291	0.874998	-0.13353	1.049824	1.590643	0.944155	63.5
2.6	0.955511	0.874998	-0.13353	1.089045	1.650068	0.950535	66.04
2.7	0.993252	0.874998	-0.13353	1.126785	1.70725	0.956112	68.58
2.9	1.064711	0.874998	-0.13353	1.198244	1.815521	0.965278	73.66
3.1	1.131402	0.874998	-0.13353	1.264936	1.916569	0.972354	78.74
3.3	1.193922	0.874998	-0.13353	1.327456	2.011297	0.977853	83.82
3.6	1.280934	0.874998	-0.13353	1.414467	2.143132	0.983949	91.44
3.9	1.360977	0.874998	-0.13353	1.49451	2.264409	0.988226	99.06
4.15	1.423108	0.874998	-0.13353	1.556642	2.358548	0.990827	105.41
4.42	1.48614	0.874998	-0.13353	1.619673	2.45405	0.992937	112.268
6	1.791759	0.874998	-0.13353	1.925293	2.91711	0.998234	152.4
9	2.197225	0.874998	-0.13353	2.330758	3.531451	0.999793	228.6
12	2.484907	0.874998	-0.13353	2.61844	3.967333	0.999964	304.8
15	2.70805	0.874998	-0.13353	2.841584	4.30543	0.999992	381
18	2.890372	0.874998	-0.13353	3.023905	4.581674	0.999998	457.2
21	3.044522	0.874998	-0.13353	3.178056	4.815236	0.999999	533.4
24	3.178054	0.874998	-0.13353	3.311587	5.017556	1	609.6
27	3.295837	0.874998	-0.13353	3.42937	5.196016	1	685.8

Appendix 2: Pushover curve for different models.

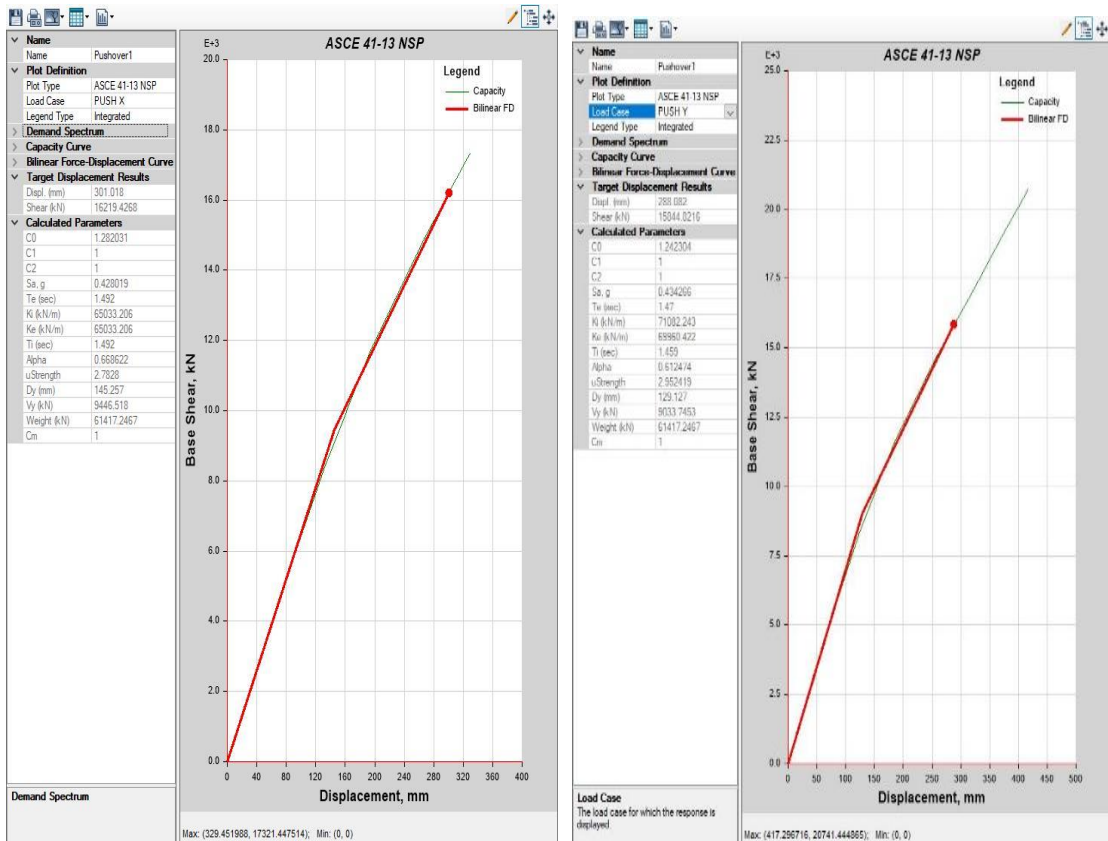


Fig. A.2.1 Pushover curves for Bare Frame structure in X and Y direction.

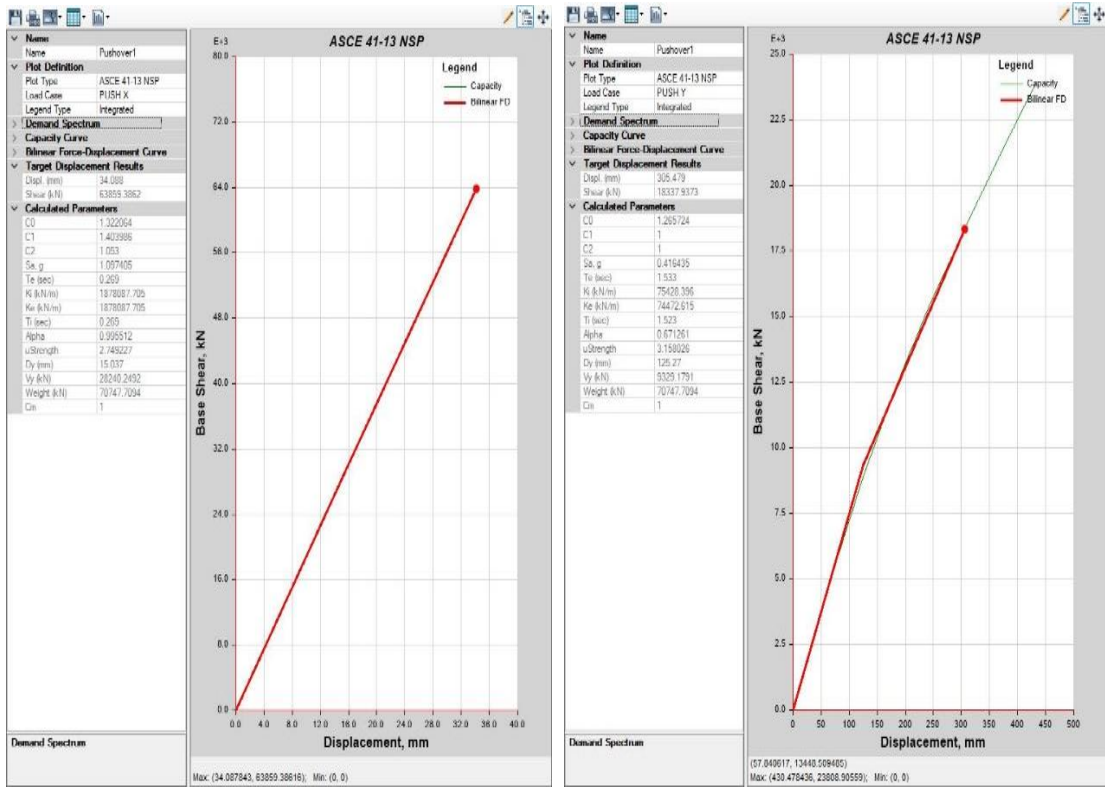


Fig. A.2.2 Pushover curves for Shear wall frame structure in X and Y direction.

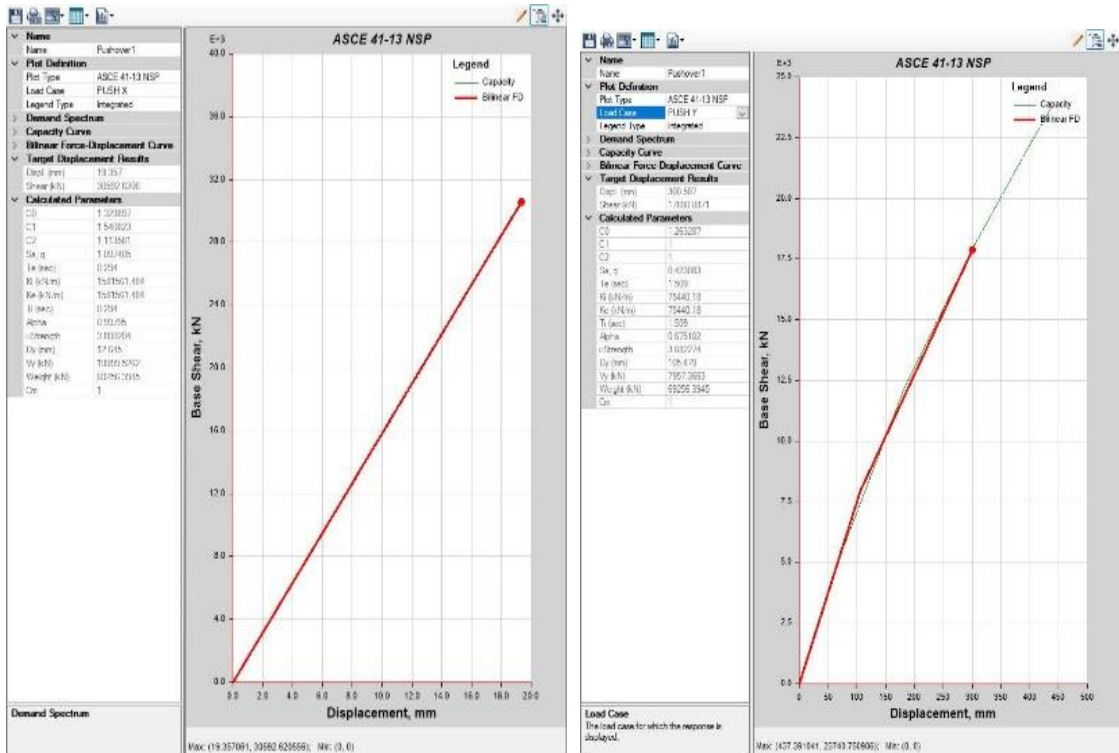


Fig. A.2.3 Pushover curves for Perforated shear wall frame structure in X and Y direction.

Appendix 3: Probability of exceedance calculation for time history results.

- a) In order to develop the fragility curves, at least three earthquakes or ground motions are required. For this analysis, the ground motions Altadena (GM1), Holliste (GM2), and S_Monica (GM3) have been selected.
- b) The top storey of the building is evaluated using time history analysis, and the results are then converted into a percentage of the Inter Story Drift Ratio (%ISDR).
- c) To assess the building's performance, interpolation is performed at the values of 0.5%, 1%, 1.5%, 2%, and 2.5% interstorey drift ratios for the Operational (OP), Immediate Occupancy (IO), Damage Control (DC), Life Safety (LS), and Collapse Prevention (CP) performance levels, respectively.
- d) To determine the fragility curves, two main parameters are evaluated: the mean (μ) and the standard deviation (σ). These parameters provide statistical measures of the damage states and their associated probabilities.
- e) Finally, the fragility curves are plotted using the standard normal cumulative distribution function. This function allows for the representation of the probability of each damage state occurring at different levels of interstorey drift ratio.

Calculation of probability of exceedance calculation for time history results for model C - PSW.

Table A.3.1 PGA AND ISDR

GM1			GM2			GM3		
PGA(g)	TSD	%ISDR	PGA(g)	TSD	%ISDR	PGA(g)	TSD	%ISDR
0	0	0	0	0	0	0	0	0
0.1	725.395	2.417983	0.1	312.868	1.042893	0.1	268.522	0.895073
0.2	1452.984	4.84328	0.2	625.774	2.085913	0.2	537.532	1.791773

Table A.3.2 Interpolation of OP, IO, DC, LS, and CP damage state

Damage State	DM	GM1	GM2	GM3
OP	0.5	0.020698	0.047943	0.055841
IO	1	0.041345	0.095883	0.111652
DC	1.5	0.061992	0.143824	0.167462
LS	2	0.082639	0.191765	0.223273

CP	2.5	0.103286	0.239705	0.279083
-----------	-----	----------	----------	----------

Table A.3.3 Mean and Standard Deviation Calculation

Mean	x1	x2	x3	SUM	SUM/N	STDEV
0.041494	0.000432	4.16E-05	0.000206	0.00068	0.000227	0.015054
0.08296	0.001732	0.000167	0.000823	0.002722	0.000907	0.030122
0.124426	0.003898	0.000376	0.001852	0.006126	0.002042	0.04519
0.165892	0.006931	0.000669	0.003293	0.010893	0.003631	0.060258
0.207358	0.010831	0.001046	0.005144	0.017022	0.005674	0.075326

Table A.3.4 Mean and Standard Deviation

Damage State	Mean	STDEV
OP	0.041494	0.015054
IO	0.08296	0.030122
DC	0.124426	0.04519
LS	0.165892	0.060258
CP	0.207358	0.075326

Table A.3.5 Probability of exceedance calculation for Model C – PSW.

PGA	OP	IO	DC	LS	CP
0.00	0.00	0.00	0.00	0.00	0.00
0.01	0.02	0.01	0.01	0.00	0.00
0.02	0.08	0.02	0.01	0.01	0.01
0.03	0.22	0.04	0.02	0.01	0.01
0.04	0.46	0.08	0.03	0.02	0.01
0.05	0.71	0.14	0.05	0.03	0.02
0.06	0.89	0.22	0.08	0.04	0.03
0.07	0.97	0.33	0.11	0.06	0.03
0.08	0.99	0.46	0.16	0.08	0.05
0.09	1.00	0.59	0.22	0.10	0.06
0.10	1.00	0.71	0.29	0.14	0.08
0.11	1.00	0.82	0.37	0.18	0.10
0.12	1.00	0.89	0.46	0.22	0.12
0.13	1.00	0.94	0.55	0.28	0.15
0.14	1.00	0.97	0.63	0.33	0.19
0.15	1.00	0.99	0.71	0.40	0.22
0.16	1.00	0.99	0.78	0.46	0.26
0.17	1.00	1.00	0.84	0.53	0.31
0.18	1.00	1.00	0.89	0.59	0.36
0.19	1.00	1.00	0.93	0.66	0.41
0.20	1.00	1.00	0.95	0.71	0.46
0.21	1.00	1.00	0.97	0.77	0.51
0.22	1.00	1.00	0.98	0.82	0.57
0.23	1.00	1.00	0.99	0.86	0.62
0.24	1.00	1.00	0.99	0.89	0.67
0.25	1.00	1.00	1.00	0.92	0.71

0.26	1.00	1.00	1.00	0.94	0.76
0.27	1.00	1.00	1.00	0.96	0.80
0.28	1.00	1.00	1.00	0.97	0.83
0.29	1.00	1.00	1.00	0.98	0.86
0.30	1.00	1.00	1.00	0.99	0.89
0.31	1.00	1.00	1.00	0.99	0.91
0.32	1.00	1.00	1.00	0.99	0.93
0.33	1.00	1.00	1.00	1.00	0.95
0.34	1.00	1.00	1.00	1.00	0.96
0.35	1.00	1.00	1.00	1.00	0.97
0.36	1.00	1.00	1.00	1.00	0.98
0.37	1.00	1.00	1.00	1.00	0.98
0.38	1.00	1.00	1.00	1.00	0.99
0.39	1.00	1.00	1.00	1.00	0.99
0.40	1.00	1.00	1.00	1.00	0.99
0.41	1.00	1.00	1.00	1.00	1.00

REFERENCES

- [1] V. Keshari, G. P. Awadhiya, (2021). Study on Optimization of Multi-Story Building with Solid and Perforated Shear Wall. Design Engineering, 7040-7054.
- [2] HAZUS 5.1, HAZUS Earthquake Model Technical Manual, Department of Homeland Security, Federal Emergency Management Agency, Washington, DC, USA, 2022.
- [3] FEMA, Pre-standard, and commentary for the seismic rehabilitation of buildings, report FEMA-356, Federal Emergency Management Agency, Washington DC, USA, 2000.
- [4] IS 13920 (2016) Indian Standard Code of Practice for Ductile Detailing of Reinforced Concrete Structures Subjected to Seismic Forces. Bureau of Indian Standards, New Delhi. 10.
- [5] IS 1893 Part 1 (2016) Indian Standard Criteria for Earthquake Resistant Design of Structures. Bureau of Indian Standards. New Delhi. 2016.
- [6] IS 456 (2000) Indian Standard for Plain and Reinforced Concrete - Code of Practice, Bureau of Indian Standards, New Delhi. 2000.
- [7] L. Astriana, S. Sangadhi, E. Purwanto, S.A. Kristiawan, (2017). Assessing seismic performance of moment resisting frame -shear wall system using seismic fragility curve. SCESCM 2016 Procedia Engineering 171:1069 – 1076.
- [8] Y. N. Nazari, M. Saatcioglu, (2017). Seismic vulnerability assessment of concrete shear wall buildings through fragility analysis. Journal of Building Engineering. 12:202–209.
- [9] K. Kamath, S. Anil (2017). Fragility curves for low-rise, mid-rise, and high-rise concrete moment resisting frame building for seismic vulnerability assessment. International Journal of Civil Engineering and Technology (IJCIET), 8:10–519.
- [10] N. Deb., N. Debnath (2016) Effect of Shear Wall on Seismic Fragility of RC Frame Structures International Journal of Engineering Research & Technology (IJERT), 5:710-714.

- [11] L. Haldera, S. Paulb (2016). Seismic Damage Evaluation of Gravity Load Designed Low Rise RC Building Using Non-Linear Static Method. ICOVP. *Procedia Engineering* 144:1373 – 1380.
- [12] R. Sharma, & J. A. Amin, (2015). Effects of opening in shear walls of 30-storey building. *Journal of Materials and Engineering Structures «JMES»*, 2(1), 44-55.
- [13] S.N.A. Saruddina, F. M. Nazria, (2015). Fragility curves for low- and mid-rise buildings in Malaysia. EACEF-5. *Procedia Engineering* 125:873 – 878.
- [14] G. Muthukumar, & M. Kumar, (2014). Influence of opening locations on the structural response of shear wall. *Journal of Nonlinear Dynamics*, 2014.
- [15] M. Marius, (2013). Seismic behaviour of reinforced concrete shear walls with regular and staggered openings after the strong earthquakes between 2009 and 2011. *Engineering Failure Analysis*, 34, 537-565.
- [16] SM. Sakurai, H. Kuramoto, & T. Matsui (2012). Shear strength evaluation for RC shear walls with multi-openings based on FEM analysis. In *Proceedings of the 15th World conference on earthquake engineering*. Lisbon, Portugal (pp. 4635-4644).
- [17] L.A. Miseses, R. R. López, A. Saffar, (2007) Development of fragility curves for medium rise reinforced concrete shear wall residential buildings in Puerto Rico. *Mecanica Computacional Vol XXVI:2712-2727*.
- [18] H. Wu, & B. Li, (2003). Parametric study of reinforced concrete walls with irregular openings. In *Proc. 7th Pacific Conference on Earthquake Engineering*, Christchurch, New Zealand.

PAPER NAME

Sudhir 2k21STE21 Thesis Final .pdf

WORD COUNT

10849 Words

CHARACTER COUNT

51434 Characters

PAGE COUNT

47 Pages

FILE SIZE

1.4MB

SUBMISSION DATE

May 31, 2023 9:15 AM GMT+5:30

REPORT DATE

May 31, 2023 9:16 AM GMT+5:30

● 12% Overall Similarity

The combined total of all matches, including overlapping sources, for each database.

- 9% Internet database
- 6% Publications database
- Crossref database
- Crossref Posted Content database
- 7% Submitted Works database

● Excluded from Similarity Report

- Bibliographic material
- Small Matches (Less than 10 words)